

Uncovering the Mechanistic Insights of Cp*Co^{III}-catalyzed C–H Methylation Reactions

BACHELOR THESIS

Marta Romero Ribas

Supervised by Mónica H. Pérez Temprano
Institute of Chemical Research of Catalonia (ICIQ)



UNIVERSITAT
ROVIRA i VIRGILI

Tarragona
2023

Table of Contents

Acknowledgements	6
1. Abstract.....	7
2. Introduction	8
2.1. The Host Institution: ICIQ.....	8
2.2. Ligand-Assisted TM-Catalyzed C–H Functionalization Reactions	8
2.3. Cp*Co ^{III} -Catalyzed C–H Functionalization Reactions.....	10
2.4. Cp*Co ^{III} -Catalyzed C–H methylation Reactions	12
3. Objectives	15
4. Results and discussion	16
4.1. Model system selection and mechanistic initial studies	16
4.2. Exploration of additional methylating sources	18
4.3. Additive effects.....	20
4.3.1. The effect of silver salt	20
4.3.2. The effect of the bases	26
4.4. C–H methylation quantification	27
5. Conclusions	34
6. Outlook.....	35
7. Experimental section	36
7.1. General procedures	36
7.2. Materials and methods.....	36
7.3. Synthesis of cobalt species	38
7.3.1. Synthesis and characterization of Cp*Co(VTMS) ₂	38
7.3.2. Synthesis and characterization of 1 _{ald} -I	39
7.3.3. Synthesis and characterization of 1 _{ppy} -I.....	40
7.4. Initial mechanistic studies	41
7.5. Exploration of additional methylating sources	42
7.6. The effect of silver salts.....	43
7.7. The effect of the bases	45
7.8. Methylation quantification	45
7.9. C–Me bond-forming reaction from alternative 1 _{DG} -I systems	46

8. Bibliography 48

Abbreviations

2-PhPy	2-phenylpyridine
°C	Celsius degree
Ald	Aldehyde
Ar	Aromatic
C	Carbon
CDCl ₃	Chloroform- <i>d</i>
CD ₂ Cl ₂	Methylene chloride- <i>d</i> ₂
Cl	Chloro
Cp*	1,2,3,4,5-pentamethylcyclopentadienyl
d	Doublet
DCM	Dichloromethane
dd	Doublet of doublets
dt	Doublet of triplets
ddd	Doublet of doublet of doublets
ddq	Doublet of doublet of quartets
DMSO- <i>d</i> ₆	Dimethyl sulfoxide- <i>d</i> ₆
DG	Directing Group
H	Hydrogen
h	Hours
I	Iodine
LSF	Late-stage functionalization
m	Multiplet
Me	Methyl
MeBpin	Methyl boronic acid pinacol ester
MeLi	Methyl lithium
MeTHF	2-Methyltetrahydrofuran
<i>n</i> -BuLi	<i>n</i> -butyl lithium
NMR	Nuclear Magnetic Resonance
ppm	Parts per million
ppy	Phenylpyridine
PTFE	Polytetrafluoroethylene

rt	Room temperature
s	Singlet
t	triplet
td	Triplet of doublets
THF	Tetrahydrofuran
THF- <i>d</i> ₈	Tetrahydrofuran- <i>d</i> ₈
TM	Transition metal
VTMS	Vinyltrimethylsilane

Acknowledgements

First of all, I would like to start by thanking Prof. Mónica H. Pérez-Temprano for giving the chance to join the group again to carry out my Bachelor Thesis. Thank you for believing in myself, helping me, and your dedication throughout this time. Being part of the group is always a pleasure for me.

Sergio Barranco, thank you infinitely for guiding me during this experience, teaching me everything from the first day with patience and a passion for chemistry, making everything easier and more fun, and for supporting me in every decision I have made. I couldn't have asked for a better *copiloto* for this adventure and all the ones we have yet to experience.

Future doctor Sara López, thank you for your knowledge and for helping me in the sincerest and kind way. You are a brilliant person with infinite capabilities. Amazing things await you in this new stage.

Future doctor Jiayu Zhang, thank you for sharing all your knowledge with me and helping me with any doubts that have arisen over time. Ulunay, your presence in the laboratory makes everything much easier, I hope you continue to bring this energy for a long time. Jiale, you are the cutest person in the lab, thank you for sharing so many moments together. To the recently joined members Alfonso, Chock, and Johannes, you have great potential, and I hope you can enjoy the group as much as I have.

Last but not least, to the most personal and important part of my life: my family and friends. Friends, thank you for being with me during this time, providing me with all the necessary support, and believing in me unconditionally. Dad, mom, and Jordi, you are the fundamental pillar of my life and the best team I could have ever had. The best part of achieving new goals is sharing them with you.

1. Abstract

Over the past decade, Cp*Co^{III} catalysts have emerged as very powerful tool within directed C–H functionalization reactions. While they have shown their tremendous potential coupling a wide variety of electrophiles, the number of nucleophilic C–H couplings is very limited. This BSc thesis aims to shed light into one of these scarce transformations. To do so, we have selected direct analogues of catalytically relevant metalacyclic Cp*Co^{III} complexes, **1_{ald-I}** and **1_{ppy-I}**, to provide valuable insights into the transmetalation and reductive elimination steps involved in Cp*Co-catalyzed C–H methylation reactions. To gain a deeper understanding of the mechanism, we conducted the reactions under various conditions to assess the role of the coupling partner and/or additives involved in this transformation, and the impact of the directing group on the reaction efficiency. Our preliminary results indicate not only that the mechanistic scenario is more complex than the one proposed in the literature, but also that the nature of the directing group affects the rate of the reaction outcome.

*Durant l'última dècada, els catalitzadors de Cp*Co^{III} han sorgit com a eines molt poderoses en les reaccions de funcionalització dirigida de C–H. Tot i que han demostrat el seu enorme potencial en l'acoblament d'una gran varietat d'electròfils, el nombre d'acoblements nucleofílic de C–H és molt limitat. Aquest Treball de Fi de Grau té com a objectiu aclarir una d'aquestes escasses transformacions. Per fer-ho, hem seleccionat anàlegs directes de complexos de Cp*Co^{III} metal·lacíclicament rellevants catalíticament, **1_{ald-I}** i **1_{ppy-I}**, per proporcionar una visió valuosa dels passos de transmetallació i eliminació reductora involucrats en les reaccions de metilació de C–H catalitzades per Cp*Co. Per aconseguir una comprensió més profunda del mecanisme, hem dut a terme les reaccions en diverses condicions per avaluar el paper de la parella d'acoblements i/o additius involucrats en aquesta transformació, així com l'impacte del grup director en l'eficiència de la reacció. Els nostres resultats preliminars indiquen no només que l'escenari mecanístic és més complex del que es proposa a la literatura, sinó també que la naturalesa del grup director afecta la velocitat del resultat de la reacció.*

2. Introduction

2.1. The Host Institution: ICIQ

Founded in 2000 by the Generalitat de Catalunya, the Institut Català d'Investigació Química (ICIQ) is a chemical research institute situated in Tarragona. In 2004, ICIQ started its research activities focused in two main areas: renewable energies and catalysis. Its primary aim is to develop new knowledge and technologies that can eventually enhance the quality of life in society.

This Bachelor (BSc) thesis has been carried out under the supervision of Prof. Mónica H. Pérez-Temprano, Senior Group Leader at ICIQ. Her research group exploits reaction mechanisms as a very powerful reaction design tool in the context of transition metal (TM) homogeneous catalysis.¹ Its goal is not only to streamline the development of more sustainable synthetic methodologies yet to unlock new reaction modes currently unprecedented in TM catalysis. Within the current on-going research lines in the group, the investigation of Cp*Co-catalyzed C–H functionalization reactions² is of particular interest and this BSc thesis is framed in this topic.

2.2. Ligand-Assisted TM-Catalyzed C–H Functionalization Reactions

The chemical community is constantly seeking for new sustainable methodologies that enable the access to highly demanded building blocks, such as pharmaceuticals and agrochemicals. In this context, transition metal catalysis has provided innovative synthetic methods for forming chemical bonds since the second half of the twentieth century, such as the palladium-catalyzed cross-couplings of organohalides with nucleophilic partners (Figure 1a).³

1 Sanjosé-Orduna, J.; Mudarra, A. L.; Martínez de Salinas, S.; Pérez-Temprano, M. H. *ChemSusChem* **2019**, *12*, 2882.

2 (a) Sanjosé-Orduna, J.; Gallego, D.; Garcia-Roca, A.; Martin, E.; Benet-Buchholz, J.; Pérez-Temprano, M. H. *Angew. Chem. Int. Ed.* **2017**, *56*, 12137. (b) Sanjosé-Orduna, J.; Sarria Toro, J. M.; Pérez-Temprano, M. H. *Angew. Chem. Int. Ed.* **2018**, *57*, 11369. (c) Sanjosé-Orduna, J.; Benet-Buchholz, J.; Pérez-Temprano, M. H. *Inorg. Chem.* **2018**, *58*, 10569. (d) Martínez de Salinas, S.; Sanjosé-Orduna, J.; Odena, C.; Barranco, S.; Benet-Buchholz, J.; Pérez-Temprano, M. H. *Angew. Chem. Int. Ed.* **2020**, *59*, 6239. (e) López-Resano, S.; Martínez de Salinas, S.; Garcés-Pineda, F. A.; Moneo-Corcuera, A.; Galán-Mascarós, J. R.; Maseras, F.; Pérez-Temprano, M. H. *Angew. Chem. Int. Ed.* **2021**, *60*, 11217.

3 (a) *Cross-Coupling Reactions: A Practical Guide*; Miyaura, N., (Ed.) in *Topics in Current Chemistry Series 2019*; Springer-Verlag Berlin Heidelberg, 2002. (b) Johansson Seechurn, C. C. C.; Kitching, M.

While these reactions are among the most used in drug discovery and development,⁴ the chemical community is after more sustainable alternatives. In this context, directed transition metal-catalyzed C–H functionalization reactions have become a cornerstone in modern synthetic organic chemistry due to their tremendous versatility to build added-value complex structures in a more environmentally friendly and atom-economical way (Figure 1b).⁵ These transformations can control the site selectivity of the C–H activation step by exploiting the coordinating ability of Lewis basic moieties in the substrates that act as directing groups.

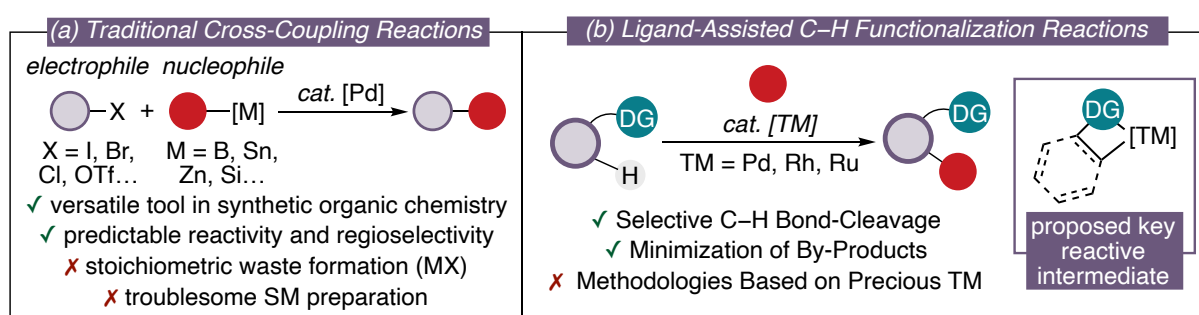


Figure 1. Pd-catalyzed cross-couplings versus TM-catalyzed C–H functionalizations.

For several decades, the catalytic systems have relied on expensive noble transition metals such as palladium (Pd), ruthenium (Ru), rhodium (Rh) or iridium (Ir). Nevertheless, first-row transition metals like cobalt have emerged as a more sustainable, attractive, and cost-effective alternative.⁶ Besides being abundant and inexpensive (cobalt costs around \$0.03 per gram compared to \$222 per gram for rhodium),⁷ cobalt catalysts offer a diverse range of reactivity patterns. They not only mimic the behavior of precious metals but also exhibit unique and

O.; Colacot, T. J.; Snleckus, V. *Angew. Chem. Int. Ed.* **2012**, *51*, 5062. (c) *Metal-Catalyzed Cross-Coupling Reactions and More*, 1st ed.; de Meijere, A., Bräse, S., Oestreich, M. (Eds.); Wiley-VCH, 2014.

4 (a) *Organometallics as Catalysts in the Fine Chemical Industry*; Beller, M., Blaser, H.-U. (Eds.); Springer-Verlag Berlin Heidelberg, **2012**. (b) *Applied Cross-Coupling Reactions*; Nishihara, Y. (Ed.); Springer-Verlag Berlin Heidelberg, **2013**.

5 (a) Labinger, J. A.; Bercaw, J. E. *Nature* **2002**, *417*, 507; (b) Bergman, R. G. *Science* **1984**, *223*, 902. (c) Hartwig, J. F. *Acc. Chem. Res.* **2012**, *45*, 864; (d) Kuhl, N.; Hopkinson, M. N.; Wencel-Delord, J.; Glorius, F. *Angew. Chem. Int. Ed.* **2012**, *51*, 10236. (e) Yamaguchi, J.; Yamaguchi, A. D.; Itami, K. *Angew. Chem. Int. Ed.* **2012**, *51*, 8960. (f) Gensch, T.; Hopkinson, M. N.; Glorius, F.; Wencel-Delord, J. *Chem. Soc. Rev.* **2016**, *45*, 2900. (g) Gunsalus, N. J.; Koppaka, A.; Park, S. H.; Bischof, S. M.; Hashiguchi, B. G.; Periana, R. A. *Chem. Rev.* **2017**, *117*, 8521.

6 Gandeepan, P.; Müller, T.; Zell, D.; Cera, G.; Warratz, S.; Ackermann, L. *Chem. Rev.* **2019**, *119*, 2192.

7 <https://www.dailymetalprice.com/> accessed on 31/05/2023.

versatile reactivity due to its low electronegativity, hard nature and the ability to access multiple oxidation states through 1- or 2-electron processes. The first example of chelation-assisted transition-metal catalyzed C–H functionalization utilizing a cobalt catalyst was reported by Murahashi in the 1950s.⁸ However, despite this early discovery, the tremendous potential of cobalt in facilitating directed C–H functionalization reactions remained largely unexplored for over 50 years. It is only in recent times that cobalt has experienced a renaissance as a promising tool in organic synthesis,⁶ thanks to the utilization of Cp*Co^{III} complexes.

2.3. Cp*Co^{III}-Catalyzed C–H Functionalization Reactions

The use of pentamethylcyclopentadienyl (Cp*) cobalt complexes, analogous to the active Rh^{III} catalysts for C–H activation⁹ and known since the mid-70s,¹⁰ has represented a significant advancement in cobalt catalysis, propelling the field forward and opening up new opportunities in organic synthesis. Since the seminal work by Kanai and Matsunaga in 2013,¹¹ numerous research groups have showcased the potential of Cp*Co^{III} complexes in driving C–C and C–heteroatom bond-forming reactions, particularly when employing electrophilic coupling partners.⁶ This distinct behavior can be attributed to the unique nature of the Cp*Co^{III}–C bond in the putative cobaltacycle formed after the C–H activation step (Figure 2).¹² In comparison to rhodium, cobalt exhibits lower electronegativity, resulting in a more polarized Co–C bond than the one present analogous metalacyclic Cp*Rh^{III} intermediates. Consequently, the increased nucleophilicity of the A-type intermediates in Figure 2 enables the reaction with less electrophilic moieties.

8 Murahashi, S. *J. Am. Chem. Soc.* **1955**, *77*, 6403.

9 (a) Colby, D. A.; Tsai, A. S.; Bergman, R. G.; Ellman, J. A. *Acc. Chem. Res.* **2012**, *45*, 814. (b) Song, G.; Li, X. *Acc. Chem. Res.* **2015**, *48*, 1020.

10 Roe, D. M.; Maitlis, P. M. *J. Chem. Soc. A* **1971**, 3173.

11 Yoshino, T.; Ikemoto, H.; Matsunaga, S.; Kanai, M. *Angew. Chem. Int. Ed.* **2013**, *52*, 2207.

12 Ikemoto, H.; Yoshino, T.; Sakata, K.; Matsunaga, S.; Kanai, M. *J. Am. Chem. Soc.* **2014**, *136*, 5424.

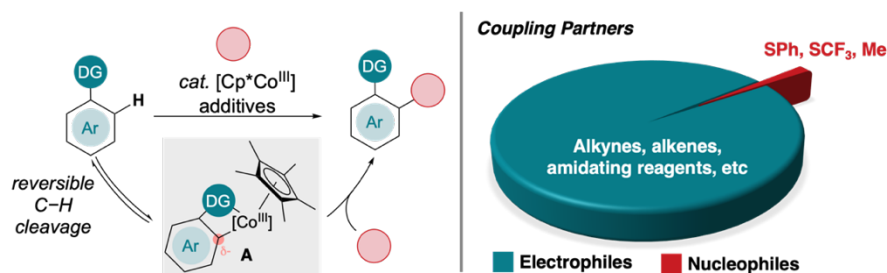


Figure 2. Cp*Co^{III}-catalyzed directed C–H functionalization reactions.

On the contrary, the use of nucleophilic coupling partners, which are commonly used in cross-coupling reactions, remains underexplored,¹³ with only three examples reported in the literature so far. In 2016, Glorius and co-workers demonstrated the oxidative coupling of indoles with thiols.¹⁴ The following year, Wang used a silver nucleophile, AgSCF₃, for the *ortho*-trifluoromethylthiolation of arenes containing monodentate directing groups.¹⁵ Indeed, recent studies performed by our group suggest that Cp*Co^{III}-catalyzed C–S nucleophilic couplings occur through oxidatively-induced reductive elimination (ORE) events involving high-valent cobalt intermediates.^{2e} Last but not least, in 2020, Ackermann and co-workers developed a very elegant synthetic methylation protocol,¹⁶ that it will further discussed in the following section.

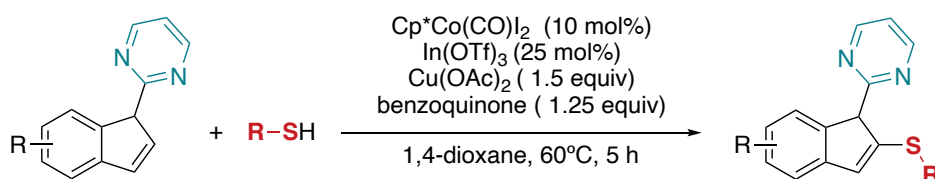
13 Barranco, S.; Zhang, J.; López-Resano, S.; Casnati, A.; Pérez-Temprano, M. H. *Nat. Synth.* **2022**, *1*, 841.

14 Gensch, T.; Klauck, F. J. R.; Glorius, F. *Angew. Chem. Int. Ed.* **2016**, *55*, 11287.

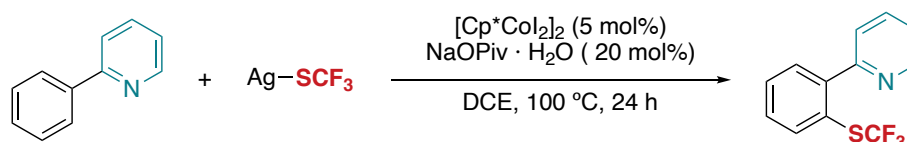
15 Liu, X. G.; Li, Q.; Wang, H. *Adv. Synth. Catal.* **2017**, *359*, 1942.

16 Friis, S.D.; Johansson, M.J.; Ackermann, L. *Nat. Chem.* **2020**, *12*, 511.

(a) *Glorius, 2016*



(b) *Wang, 2017*



(c) *Pérez-Temprano, 2021*

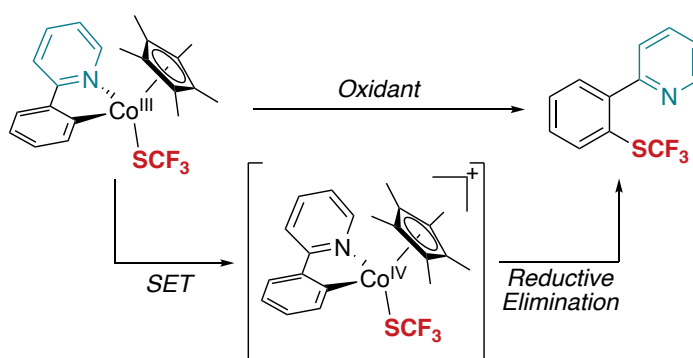


Figure 3. Nucleophiles scheme reactivity.

2.4. Cp*Co^{III}-Catalyzed C–H methylation Reactions

Late-stage functionalization (LSF) is a valuable strategy in drug development, allowing for the construction and diversification of complex molecules.¹⁷ C–H methylation, the process of replacing a hydrogen atom with a methyl group, holds significant potential for enhancing the potency and pharmacokinetic properties of lead molecules due to the so-called “magic methyl effect”.¹⁸ However, existing methods for transition-metal-catalyzed C–H activation and methylation in LSF are challenging, limited in scope and rely on noble metal catalysts.¹³ To address these limitations, Ackermann and co-workers proposed a novel approach catalyzed by Cp*Co^{III} complexes and that utilizes a boron-based methyl source.¹⁶ This approach allowed the direct diversification of lead molecules by leveraging the inherent functional groups already

17 (a) Guillemard, L.; Kaplaneris, N.; Ackermann, L.; Johanson, M. J. *Nat. Rev. Chem.* **2021**, *5*, 522.

(b) Zhang, L.; Ritter, T. *J. Am. Chem. Soc.* **2022**, *144*, 2399.

18 Aynedinova, D.; Callens, M. C.; Hicks, H. B.; Poh, C. Y. X.; Shennan, B. D. A.; Boyd, A. M.; Lim, Z. H.; Leitch, J. A.; Dixon, D. J. *Chem. Soc. Rev.* **2021**, *50*, 5517.

present in the molecules themselves. In addition, the mild conditions employed in this methodology allows broad functional group tolerance, accommodating the polyfunctional nature of modern pharmaceutical agents.

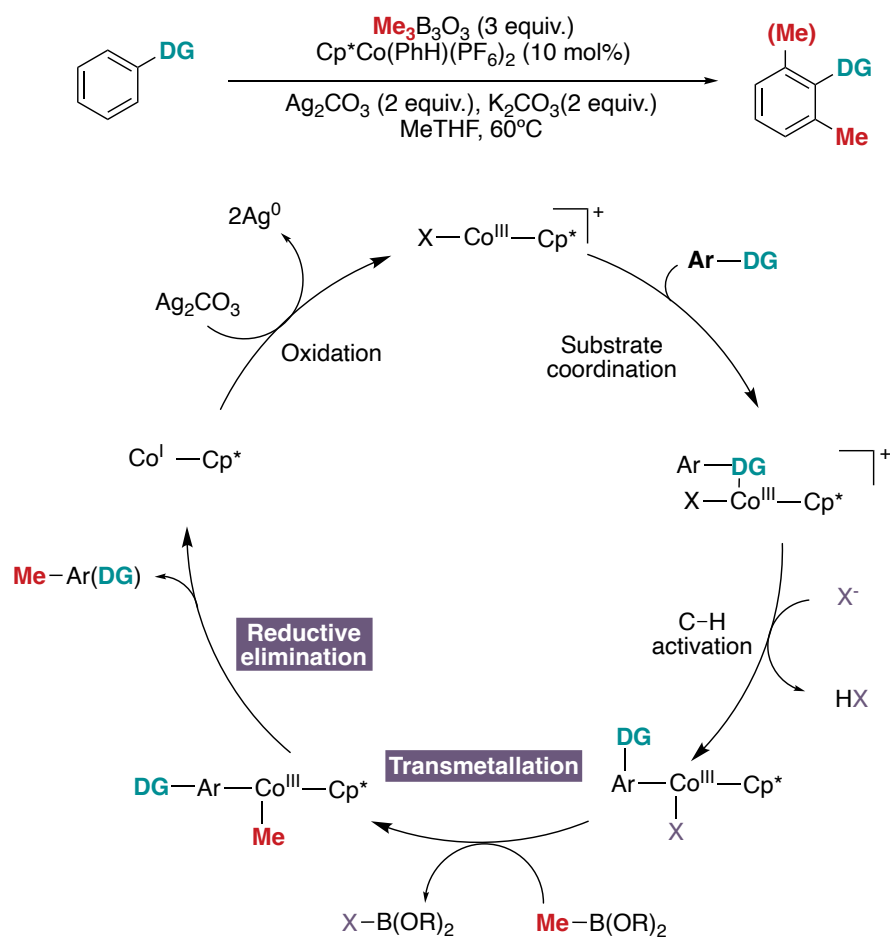


Figure 4. Cp*Co-catalyzed C–H methylation reaction and mechanistic proposal.

In Figure 4, it is shown the catalytic cycle, composed by several elementary steps, proposed by the authors. First, after the coordination of the organic substrate to the cobalt center, the C–H activation takes place. The resulting cobaltacyclic intermediate undergoes transmetalation in which a methyl group is transferred from the trimethylboroxine to the cobalt(III) metal center to afford a methylated cobaltacycle. Upon reductive elimination of the C–Me bond, the methylated organic product is formed along with a low oxidation state cobalt complex. Oxidation of the resulting Co^I species regenerates the active Co^{III} species.

Prompted by our group interests on nucleophilic coupling and intrigued by the proposed mechanism for the methylation protocol, we intend to gain a deeper mechanistic understanding of this catalytic system. In particular, we focused our attention to two of the less explored elementary steps within Cp*Co catalytic cycles: the transmetalation and the reductive elimination. These elementary steps have been extensively studied in noble metal catalysts, especially in palladium.¹⁹ However, the factors that determine their success or failure in these Cp*Co-based systems remain completely unknown. In particular, we wanted to unravel the role of the employed additives, especially the silver salts, in the above-mentioned organometallic steps. Despite silver salts are proposed to act merely as halide scavengers or terminal oxidizing reagents to regenerate the active species after the bond-forming reaction, they can play alternative major roles, such as transmetalating agents,²⁰ or facilitating oxidative induced reductive elimination events, via high-valent organometallic species, as our group recently reported.^{2e}

19 (a) *Organotransition Metal Chemistry: From Bonding to Catalysis*, 1st ed.; Hartwig, J. F. (Ed.); Palgrave Macmillan, **2009**. (b) *Organometallics in Synthesis, Third Manual*; Schlosser, M. (Ed.); Wiley, **2013**. (c) *The Organometallic Chemistry of the Transition Metals*, 7th ed.; Crabtree, R. H. (Ed.); Wiley, **2019**.

20 Mudarra, A. L.; Martínez de Salinas, S.; Pérez-Temprano, M. H. *Org. Biomol. Chem.* **2019**, *17*, 1655.

3. Objectives

The main objective of this Bachelor Thesis is to gain a deeper mechanistic insight into Cp*Co-catalyzed nucleophilic C–H methylation couplings. The following objectives are proposed:

1. Design and synthesize catalytically relevant cobaltacyclic species to study the transmetalation and reductive elimination steps.
2. Investigate the transmetalation step with trimethylboroxine under different reaction conditions.
3. Study the mechanisms of the C–Me bond-forming reaction, via direct coupling or oxidatively induced reductive elimination events, including the synthesis and isolation of putative methylated cobaltacyclic intermediates.

4. Results and discussion

4.1. Model system selection and mechanistic initial studies

According to the mechanistic proposal depicted in Figure 5, the nucleophilic C–Me coupling triggered by Cp*Co^{III}-based systems might occur via direct reductive elimination from cobalt(III) intermediates.¹⁶ This contrasts with our group's recent findings that demonstrated the involvement of oxidatively induced reductive elimination events are key to enable nucleophilic C–S bond-forming reactions in Cp*Co-catalyzed C–H functionalization reactions.^{2e} In the latter, the presence of silver salts are crucial to access the reactive high-valent cobalt(IV) intermediates from which the C–S coupling takes place. In order to get a deeper insight into the mechanisms of Cp*Co^{III}-catalyzed C–H methylation reactions, we started our investigation by choosing a model system which would allow us to interrogate the possible reaction pathways. We selected **1_{ald-I}** as starting point following several considerations (Figure 5). First, we targeted this compound as initial cobalt precursor since it is readily accessible via oxidative addition.^{2d} Second, prior work in our lab has shown its facile participation in transmetalation reactions with nucleophilic partners,²¹ affording direct analogues of the metalacyclic intermediates, such as **B**, that can be involved in C–Nuc couplings. Finally, the aldehydic proton exhibits a distinctive chemical shift in ¹H NMR spectroscopy, facilitating the mechanistic study.

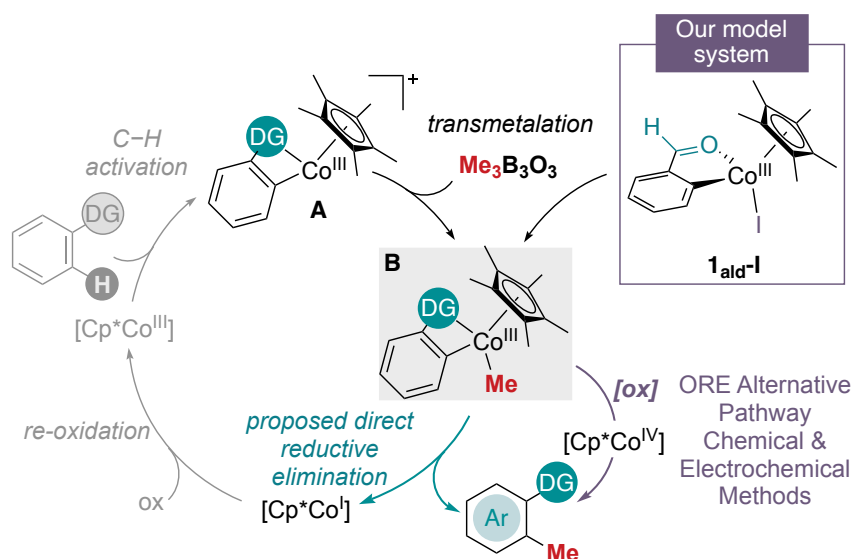
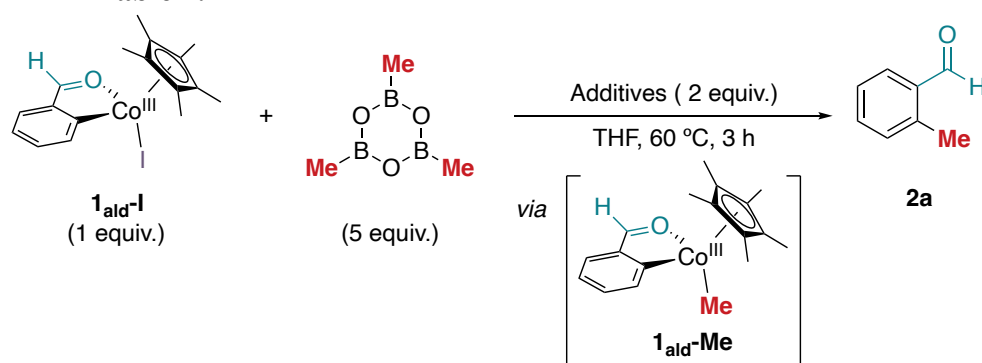


Figure 5. Model system.

21 Unpublished results by the Pérez-Temprano group.

For our initial studies, first we tested the reactivity **1_{ald-I}** with trimethylboroxine, the methylating reagents employed by Ackermann and co-workers.¹⁶ To do so, inside a glovebox under argon atmosphere, an NMR tube was charged with **1_{ald-I}** and Me₃B₃O₃ and a DMSO-*d*₆ capillary before the solvent, non-deuterated THF, was added. Thereafter, the NMR tube was taken out the glove box and heated at 60 °C for 3 hours. Due to the low quality of the NMR spectra in the non-deuterated THF, we filtrated the solution, removed the solvent, and analyzed the reaction crude again by ¹H NMR spectroscopy, but using CDCl₃ as solvent. In any of the cases we observed product derived from the C–Me bond-formation (Table 1, entry 1). This result suggests that the presence of Ag₂CO₃ and/or K₂CO₃ is crucial to promote the formation of the metacyclic Cp*Co^{III}–Me complex and the coupling product.

Table 1. Reaction conditions of the initial mechanistic studies.



Entry	Additives	Ratio (2a:1 _{ald-I})
1	None	0:100
2	K ₂ CO ₃	8:92
3	Ag ₂ CO ₃	57:43
4	Ag ₂ CO ₃ and K ₂ CO ₃	21:79

To provide further evidence for this hypothesis, we performed the reaction between **1_{ald-I}** and Me₃B₃O₃ in the presence of one or both additives (Table 1, entries 2-4). Following a similar experimental procedure, we analyzed the reaction mixture after heating the reaction at 60 °C for 3 hours. While only trace amounts of the organic product are observed with the cocktail Me₃B₃O₃/K₂CO₃, the mixtures of Me₃B₃O₃/Ag₂CO₃ and Me₃B₃O₃/K₂CO₃/Ag₂CO₃ led to a mixture of the coupling product along with **1_{ald-I}**, in 57:43 and 21:79 ratio, respectively, by ¹H

NMR spectroscopy.²² The formation of a new cobaltacyclic species, that could be assigned as **1_{ald}-Me**, was not observed in any case, suggesting that after the methylated cobaltacycle is formed, the reductive elimination step takes place immediately. In addition, these results indicate the crucial role of the silver salt in the targeted transformation since we observed product formation in the absence of K₂CO₃.

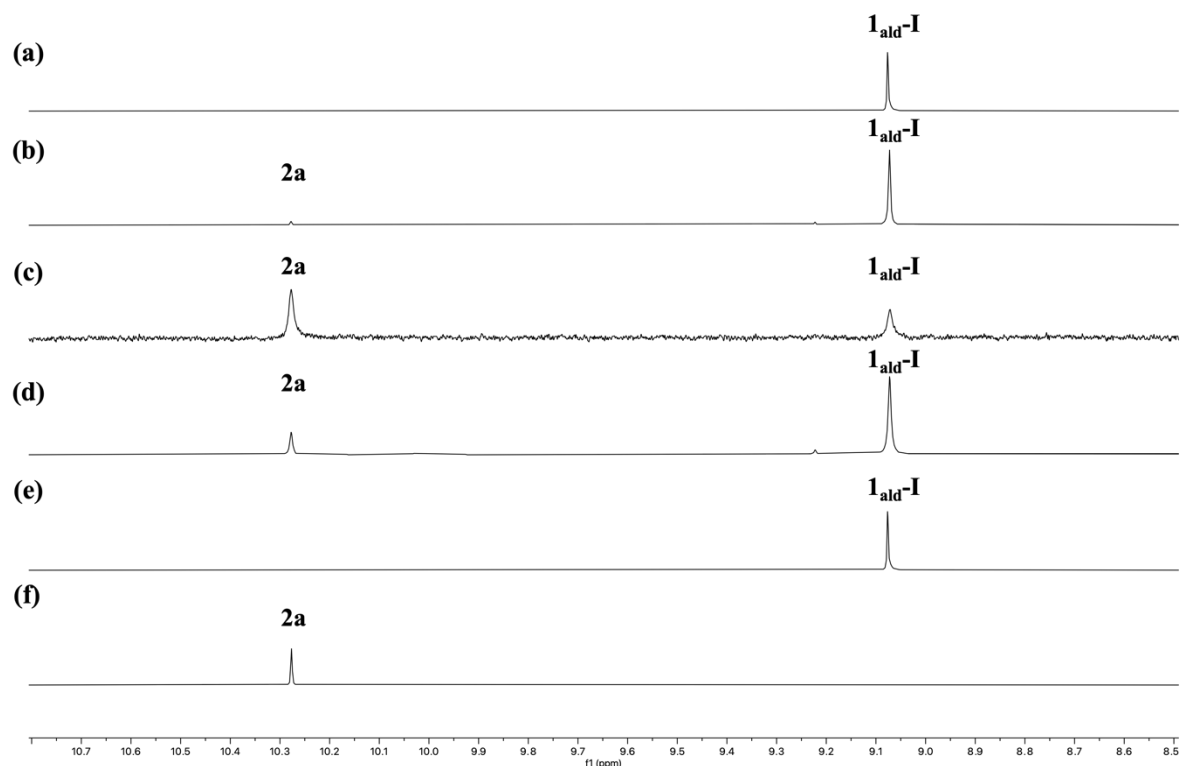


Figure 6. ¹H NMR spectra of the initial mechanistic studies. Additives: (a) No additives (Entry 1); (b) K₂CO₃ (Entry 2); (c) Ag₂CO₃ (Entry 3); (d) Ag₂CO₃ and K₂CO₃ (Entry 4). Reference NMR spectra of: (e) **1_{ald}-I**; (f) **2a**.

4.2. Exploration of additional methylating sources

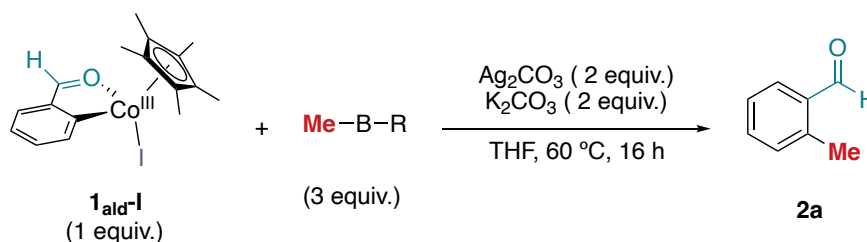
Next, we explored the reactivity of alternative commercially available methyl boron reagents (Table 2). In this case, reactions were set-up in crimped vials under inert atmosphere. Then, the mixtures were filtered and analyzed by ¹H NMR spectroscopy using CD₂Cl₂ as solvent. When MeBpin was utilized (Entry 1) neither product signal was observed or the signal of the initial cobaltacycle.²³ On the other hand, using MeBF₃K as a methyl boron reagent, we

²² We compared the obtained ¹H NMR spectra of the reaction with spectra of the initial **1_{ald}-I** and the spectra of pure **2a** and we confirmed the formation of the methylated aldehyde.

²³ Due to the lack of further experiments with this nucleophilic source, we cannot conclude why we do not observe any organic or organometallic compound by ¹H NMR spectroscopy.

observed product formation in a ratio 59:41. However, these reactions do not improve the results obtained with the Me₃B₃O₃.

Table 2. Exploration of additional methylating sources.



Entry	Reagents	Ratio (2a:1 _{ald-I})
1	MeBpin	0:100
2	MeBF ₃ K	59:41

(a)

(b)

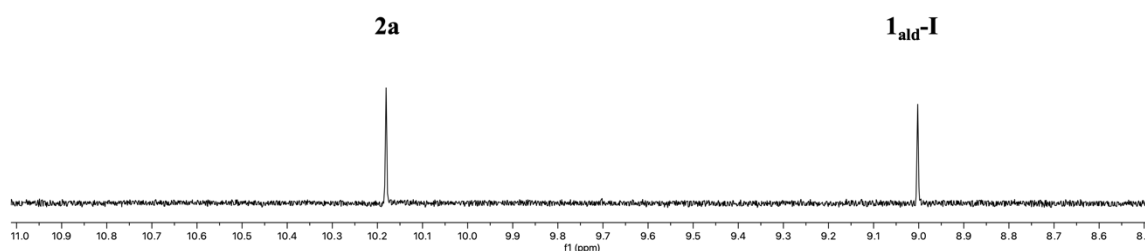


Figure 7. ¹H NMR spectra recorded using additional methylating sources: (a) MeBpin (Entry 1); (b) MeBF₃K (Entry 2).

Additionally, we explored the reactivity of **1_{ald-I}** with MeLi. This commonly used reagent has been traditionally used in organometallic chemistry to synthesize transition-metal methyl complexes.²⁴ Unfortunately, the reaction between **1_{ald-I}** and methyl lithium in THF at -78 °C

²⁴ Campos, J.; López-Serrano, J.; Peloso, R.; Carmona, E. *Chem. Eur. J.* **2016**, *22*, 6432.

for 1 hour, and then gradually warming to room temperature, did not afford **1_{ald}-Me** or the coupling product **2a** (Figure 8).

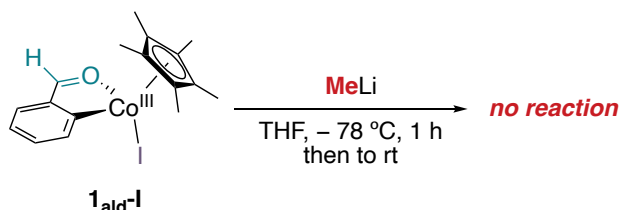


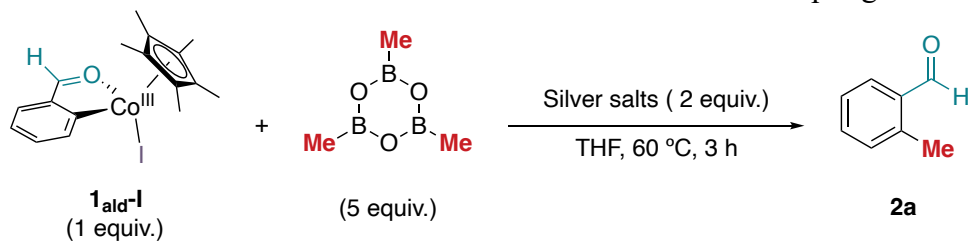
Figure 8. Unsuccessful attempt to synthesize **1_{ald}-Me** using MeLi.

4.3. Additive effects

4.3.1. The effect of silver salt

Inspired by the promising results obtained during the initial studies with the trimethylboroxine, we aimed to evaluate the effect of different widely used additives in our targeted stoichiometric C–C bond-forming reaction. First, we tested the reactivity between **1_{ald}-I** and trimethylboroxine in the presence of different silver sources (Table 3, Figure 9).

Table 3. Effect of different silver salts on the C–Me coupling.



Entry	Silver sources	Ratio (2a:1 _{ald} -I)
1	Ag ₂ CO ₃	57:43
2	AgSbF ₆	17:83
3	AgOAc	32:68
4	AgBF ₄	Decomposition

The reactions were set up in screw-cap NMR tubes under inert atmosphere in THF in the presence of a DMSO-*d*₆ capillary. As the NMR spectrum obtained in these cases were broad, the crude was filtered and ¹H NMR spectra was measured again in CDCl₃. By analyzing the reaction outcomes, we can establish that other silver sources, such as AgSbF₆ and AgOAc (entries 2 and 3) also are capable of promoting the formation of the desired product in a **2a/1_{ald}-I**

I ratio 17:83 and 32:68, respectively. However, those results are slightly worse than the ones obtained with Ag_2CO_3 (Table 3, entry 1). Unfortunately, with AgBF_4 , **1_{ald-I}** mainly suffered decomposition, only observing small amounts of **2a**.

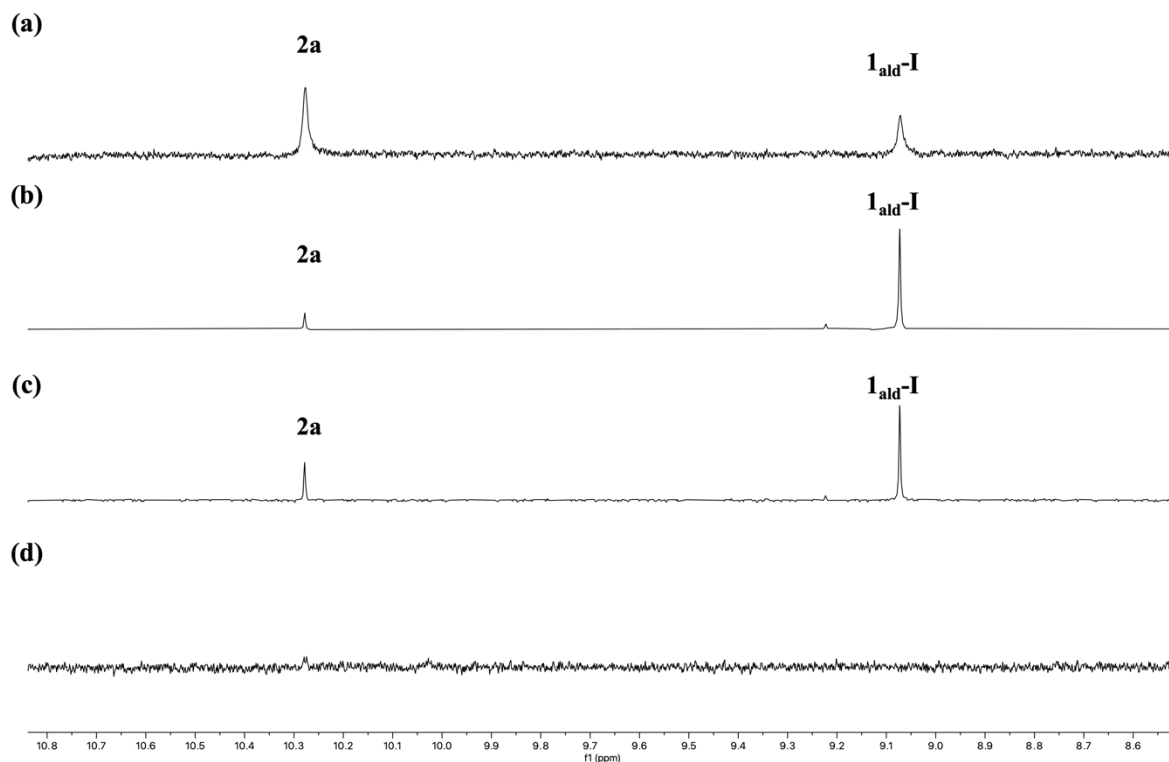


Figure 9. ^1H NMR spectra of the C–Me coupling in the presence of different silver salts. Additives: (a) Ag_2CO_3 (Entry 1); (b) AgSbF_6 (Entry 2); (c) AgOAc (Entry 3); (d) AgBF_4 (Entry 4).

After establishing that Ag_2CO_3 provides the best results in our stoichiometric reaction, we focused our attention on elucidating the exact role of silver in the C–C coupling. As mentioned in the introduction, silver salts exhibit a very versatile reactivity, serving from halide scavengers or oxidizing reagents to transmetalating agents. First, we investigated whether Ag_2CO_3 can facilitate the halide abstraction under our reaction conditions. Our group has recently demonstrated that the treatment of **1_{ald-I}** with different AgX salts ($\text{X} = \text{BF}_4, \text{NTF}_2$) in THF leads to the formation of a cationic cobaltacycle that contains a molecule of THF as ligand (Figure 9).^{2d} In sharp contrast to our previous results, when we monitored by ^1H NMR spectroscopy the reaction of **1_{ald-I}** with Ag_2CO_3 in $\text{THF-}d_8$ we do not detect the formation of **1_{ald-THF}**. Instead, we observed unreacted **1_{ald-I}** remaining and the formation of small

quantities of benzaldehyde,²⁵ that is the protodemetalation product (Table 4). Despite we used dried THF-*d*₈ for carrying out our experiments, we hypothesize that the protonation of the Co–C bond by adventitious water presence in the reaction mixture releases benzaldehyde.

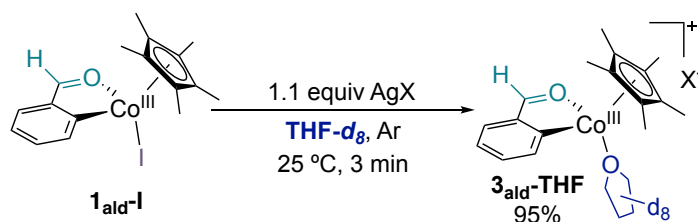
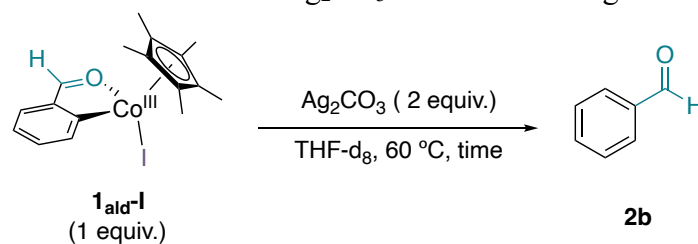


Figure 10. Previous results from the research group (*ACIE* 2020).

Table 4. Role of Ag₂CO₃ as halide scavenger.



Entry	Time	Ratio (2b:1 _{ald-I})
1	1 hour	0:100
2	3 hours	30:70

²⁵ We have confirmed the assignment of the new peak as benzaldehyde by analyzing this commercially available reagent by NMR spectroscopy.

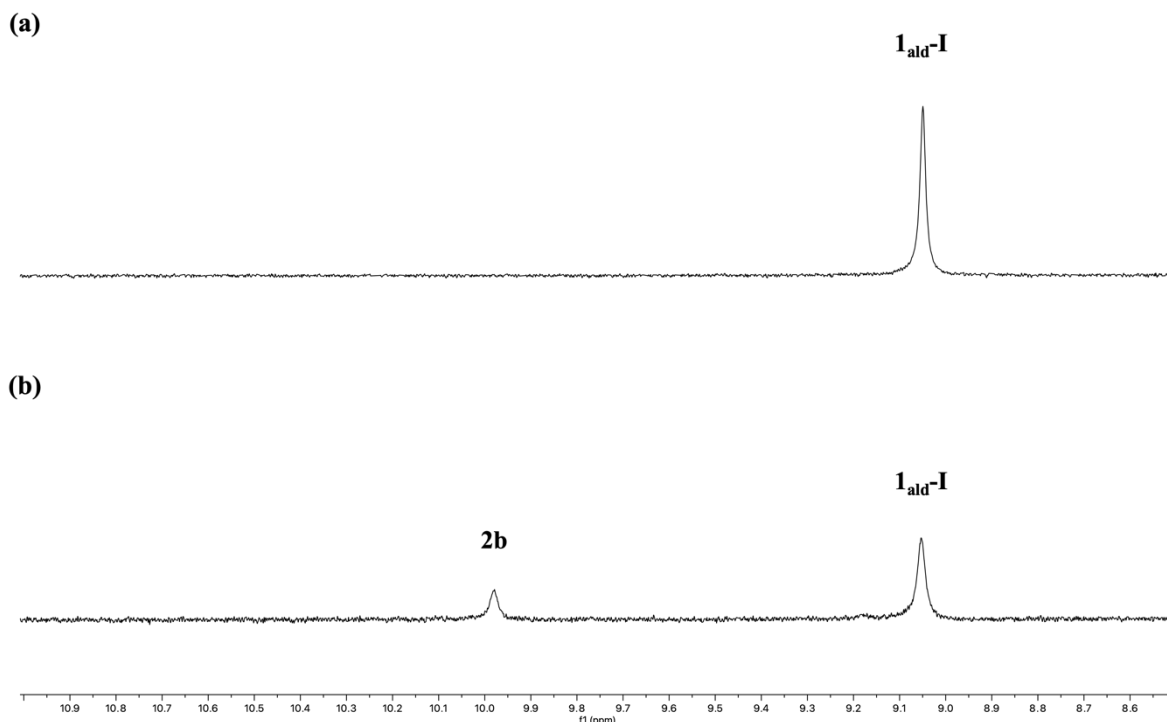


Figure 11. ^1H NMR spectra on the role of Ag_2CO_3 as halide scavenger. Time: (a) 1 hour (Entry 1); (b) 3 hours (Entry 2).

Based on our previous results, it seems that Ag_2CO_3 plays a more complex role than just been a halide scavenger, since we cannot observe the formation of $\mathbf{1}_{\text{ald-THF}}$ from $\mathbf{1}_{\text{ald-I}}$. Moreover, the direct transmetalation using trimethylboroxine, in the absence of any additional additive, also proved to be inefficient (Figure 12a). Thus, we next explore whether silver salts can play a key role in the transmetalation step. We wondered if the boron nucleophile could react with Ag_2CO_3 and form an *in situ* organometallic species, $[\text{Ag-Me}]$, that would be the reactive transmetalating agent. As mentioned before, coinage metals, especially silver, can generate nucleophilic species, that can promote innovative transformations through a transmetalation step.²⁰ Indeed, in the context of Cp^*Co -catalyzed C–H functionalization reactions, Glorius and co-workers have proposed the *in situ* generated $[\text{Cu}(\text{SPh})_2]^-$ as the active species in their C–S cross-coupling (Figure 12b).¹⁴

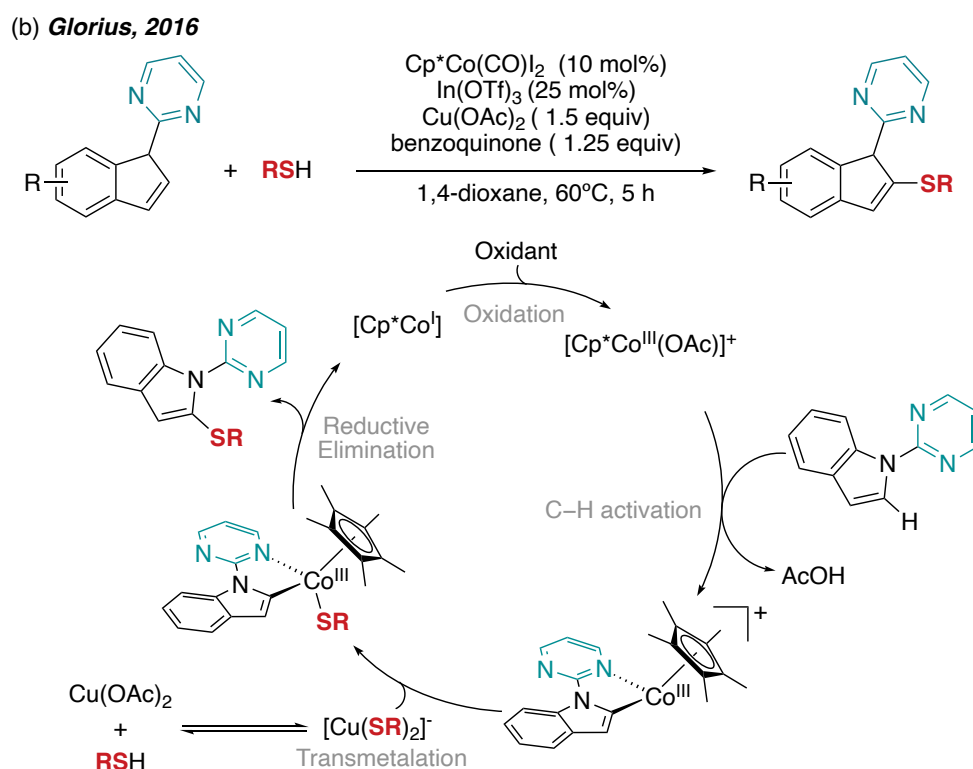
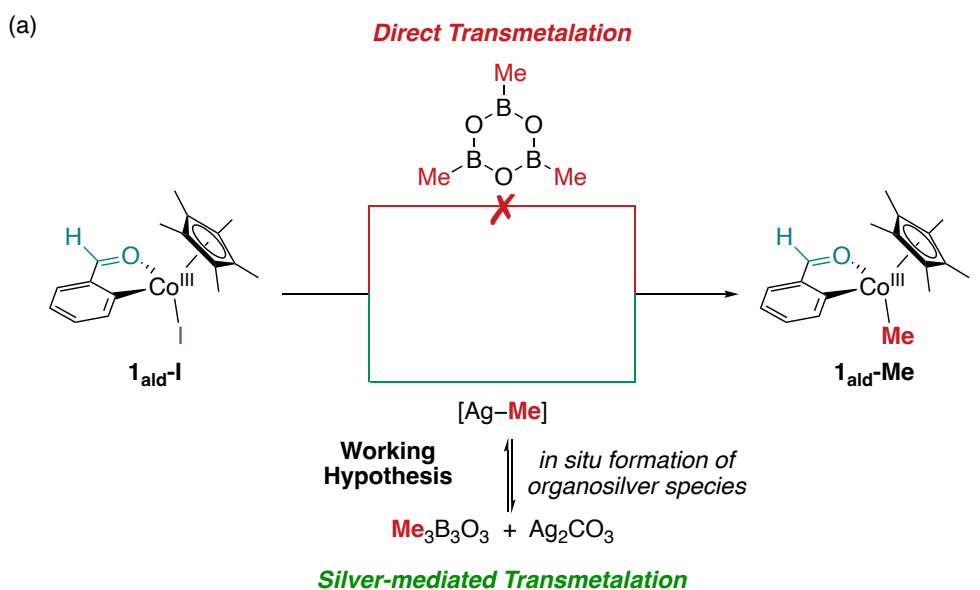


Figure 12. (a) Possible mechanistic pathways for the transmetalation step. (b) Catalytic cycle proposed by Glorius and co-workers (reference 14).

To test this hypothesis, we accessed a direct analogue of the cationic cobaltacycle that it would be formed after the C–H activation step in catalysis (Figure 13a). We employed **1_{ald}-THF**, previously reported by our group,^{2d} that contains THF as stabilizing ligand instead of I. To synthesize **1_{ald}-THF**, a vial was charged with **1_{ald}-I**, AgNTf₂ and THF under argon and the reaction was stirred at room temperature for 5 minutes (Figure 13b).

After forming the cationic cobaltacycle, we submitted the compound to two different conditions (Table 5). The mixtures were stirred for 3 hours at 60°C in both cases. According to Figure 14, we barely obtained the desired product **2a** after the experimentation using Ag_2CO_3 , $\text{Me}_3\text{B}_3\text{O}_3$ and **1ald-THF**. Furthermore, under these conditions we could form benzaldehyde, referred as **2b** product. Moreover, we could test that Ag_2CO_3 is crucial as an additive to carry out the reaction and achieve the product, otherwise the product none of the products were not observed.

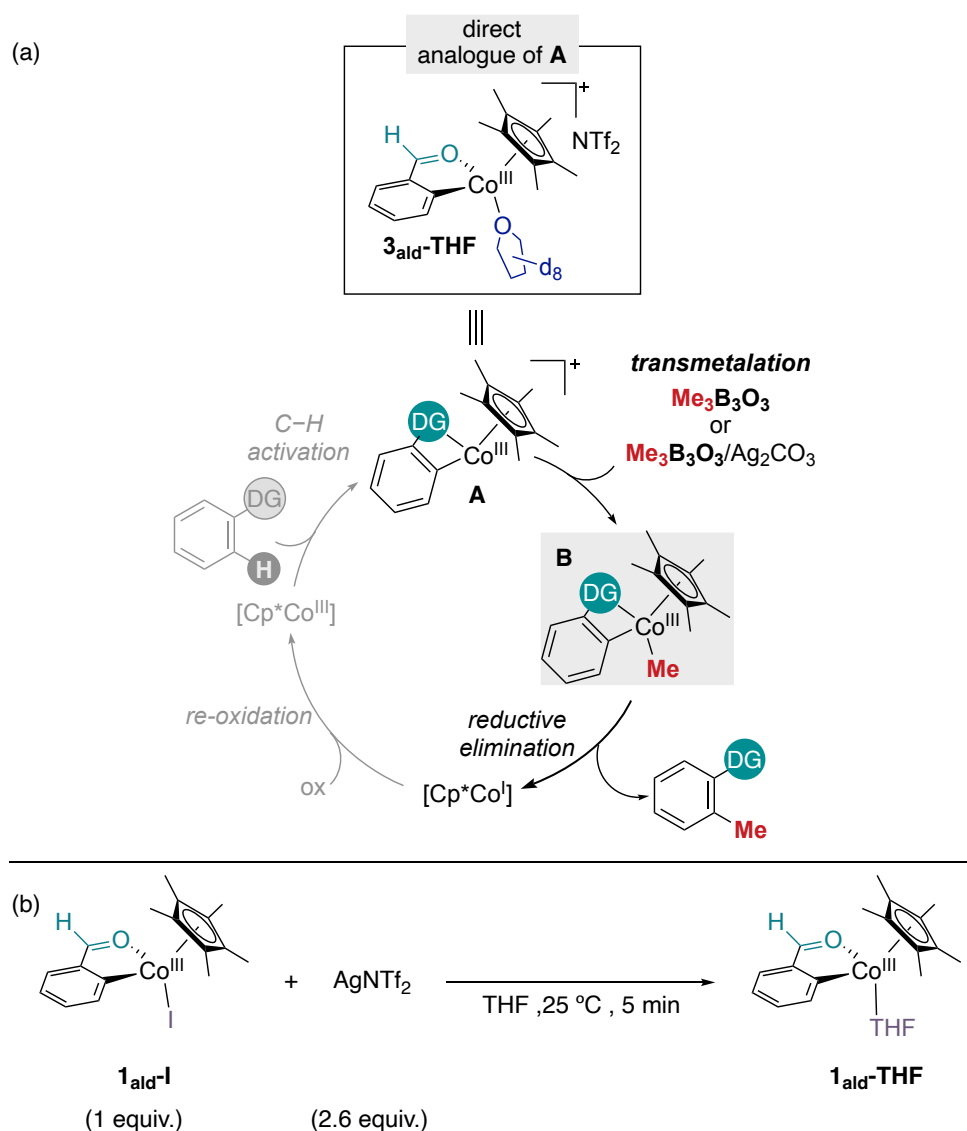
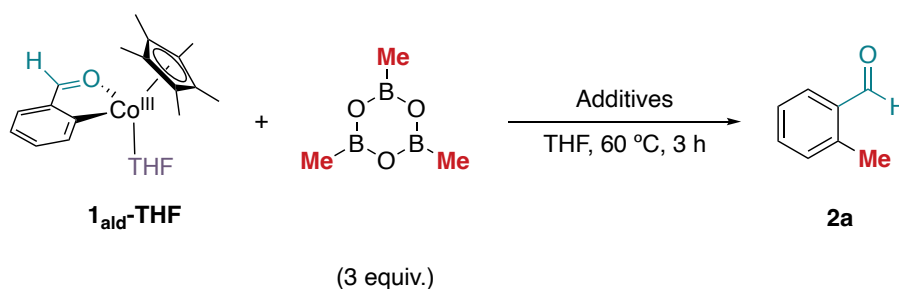


Figure 13. (a) Catalytic cycle proposed by Ackermann (reference 16). (b) Synthetic route to access **1ald-THF** previously reported by the Pérez-Temprano group.

Table 5. Study of C–Me formation using **1_{ald}-THF** as starting material



Entry	Additives	Ratio (2a:1 _{ald} -I)
1	None	0:100
2	Ag ₂ CO ₃	30:70

(a)



(b)

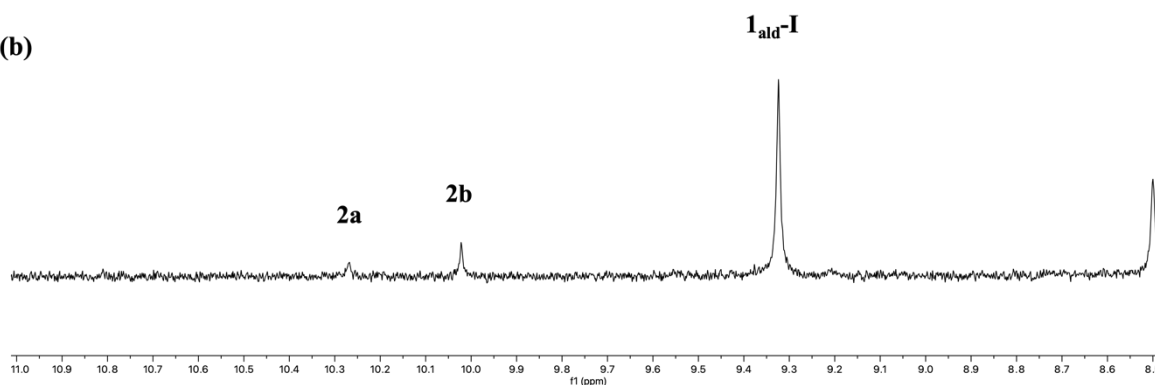


Figure 14. ¹H NMR spectra of the C–Me coupling using **1_{ald}-THF** as starting material. Additives: (a) None (Entry 1); (b) Ag₂CO₃ (Entry 2).

4.3.2. The effect of the bases

After exploring the effect of the several silver salts, we next tested the role of other potassium bases. As it is shown in Table 6, in addition to K₂CO₃, we also explored KOAc. Even though with our reference base, K₂CO₃, we observed traces of **2a** (Entry 1), in the presence of KOAc we only observed unreacted **1_{ald}-I** (Entry 2).

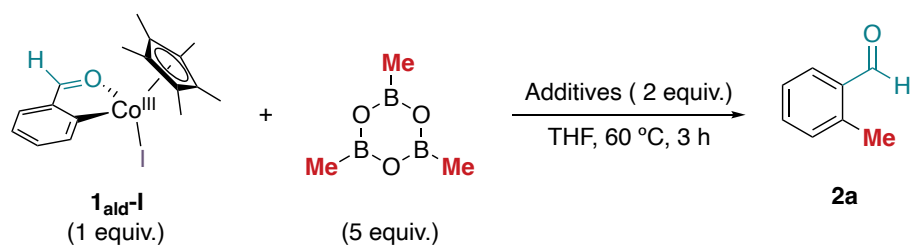


Table 6. Effect of the bases.

Entry	Additives	Ratio (2a:1 _{ald-I})
1	K ₂ CO ₃	8:92
2	KOAc	0:100

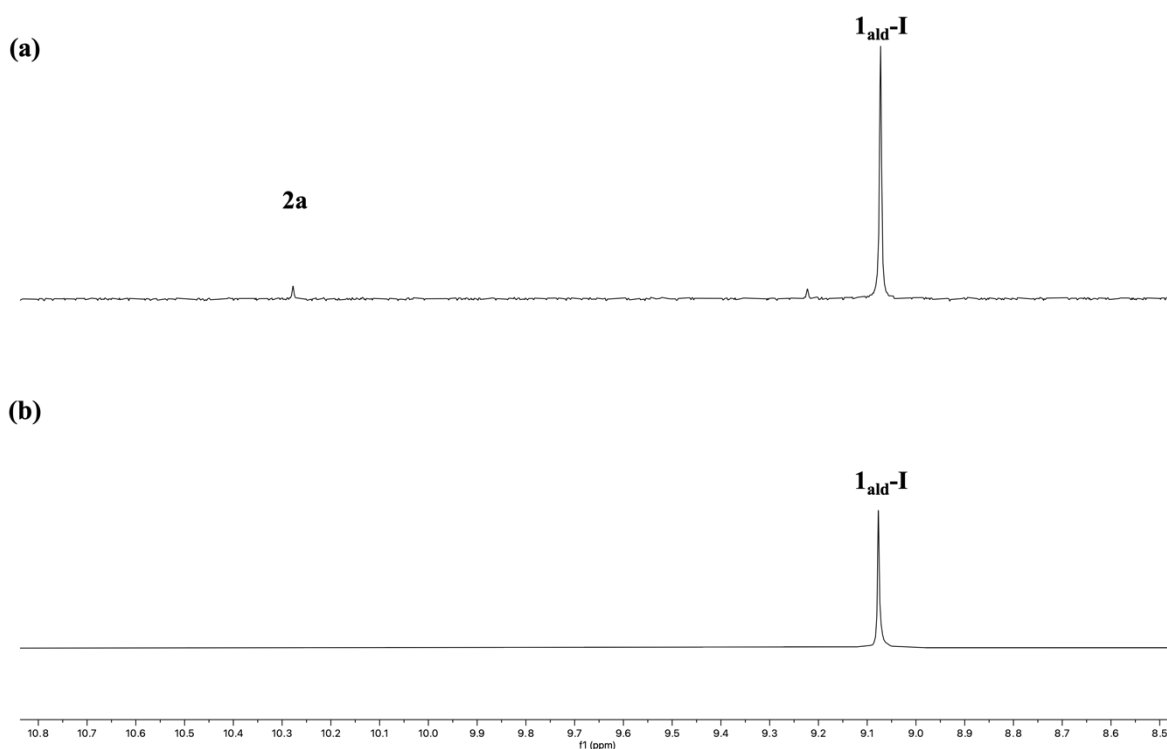


Figure 15. ¹H NMR spectra of the effect of bases. Additives: (a) K₂CO₃ (Entry 1); (b) KOAc (Entry 2).

4.4. C–H methylation quantification

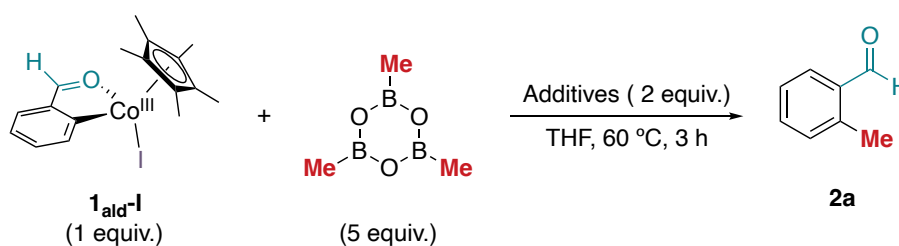
After our initial qualitative measurements, determining the ratio between the observed species, next we focused our attention in quantifying the formation of the desired organic product by ¹H NMR spectroscopy. To do so, we performed the corresponding reactions in a

non-deuterated solvent, and measured the reaction outcome by ^1H NMR spectroscopy in CDCl_3 adding a known amount of 1,3,5-trimethoxybenzene as internal standard. As shown in Figure 16, the reaction conditions using Ag_2CO_3 and $\text{Ag}_2\text{CO}_3/\text{K}_2\text{CO}_3$ as additives yielded the desired product **2a**. However, we observed the appearance of an unexpected species around 9.3 ppm, which we assigned as the chlorinated cobaltacycle **1_{ald-Cl}** according, to previous knowledge from our research group.

Following these findings and the observation of a new product that could potentially be **1_{ald-Cl}**, we synthesized the chlorinated cobaltacycle and compare its chemical shift to the one observed in the new spectra. To form **1_{ald-Cl}** we carried out the reaction in a screw cap NMR tube which was charged with a known amount of **1_{ald-I}**, $\text{Me}_3\text{B}_3\text{O}_3$, CDCl_2 instead of THF. The reaction progress was monitored using ^1H NMR spectroscopy at room temperature. After one hour, we observed the presence of compounds **2a** and **1_{ald-Cl}** in the spectra, leading us to conclude that the unexpected compound observed at 9.3 ppm was indeed **1_{ald-Cl}**, which was easily formed when using CDCl_3 or CD_2Cl_2 as solvents for the quantification.

Apart from the unexpected formation of **1_{ald-Cl}**, we found an striking result when we analysis the NMR spectra. We observed that the maximum yield measured was 25% (Entry 1) and 14% (Entry 2), despite the reaction proceeded in a smooth manner.²⁶ This clearly suggests that our reaction presents a mass-balance problem.

Table 7. C–H methylation quantification.



Entry	Additives	NMR yield
1	Ag_2CO_3 and K_2CO_3	25%
2	Ag_2CO_3	14%

²⁶ We observe the formation of additional unknown by-product at 10.6 ppm.

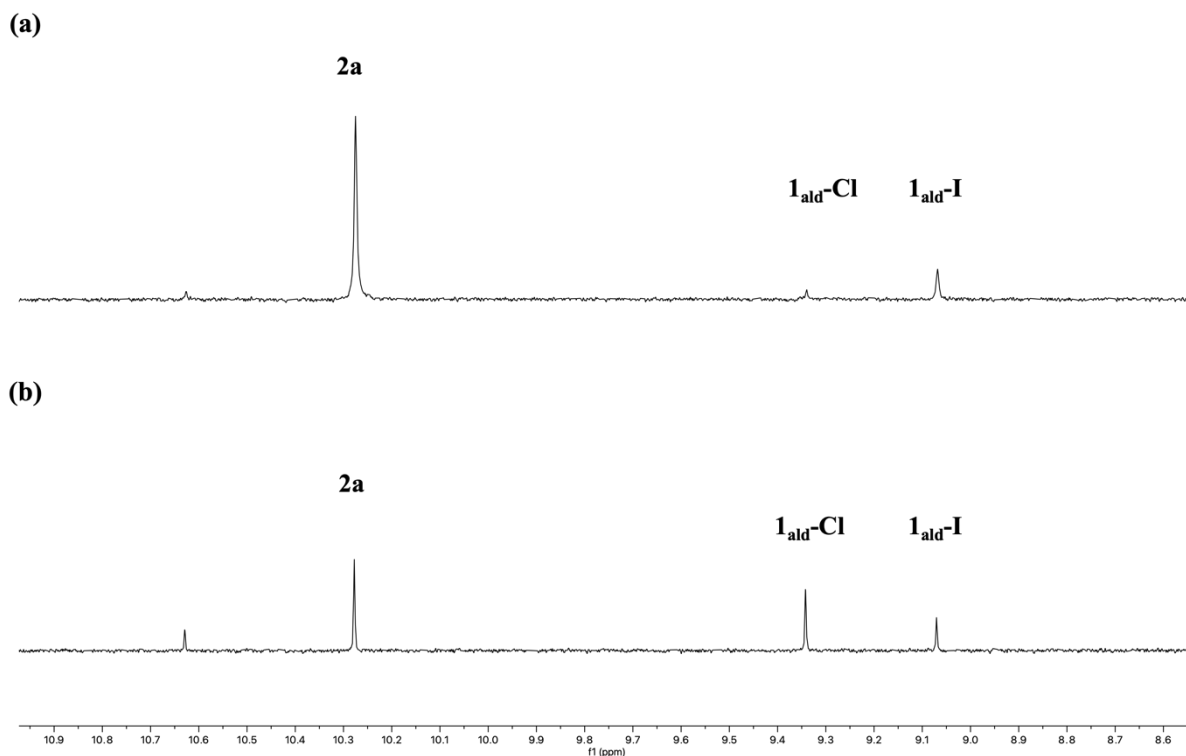


Figure 16. ^1H NMR spectra of the C–H methylation quantification Additives: (a) Ag_2CO_3 And K_2CO_3 Entry 1); (b) Ag_2CO_3 (Entry 2).

A possible explanation for this experimental observation is that there could be a problem with the work-up of the reaction. To test this hypothesis, we tested the volatility of methylated product, which is commercially available. It is worth mentioning that the boiling point of 2-methylbenzaldehyde is 200 °C and that for the reaction work-ups, we evaporated the solvent of the reaction, by using either rotatory evaporator or Schlenk line. For our test, the same amount of 2-methylbenzaldehyde (7 μL) were added in two different vials and those were subsequently weighted: vial 1 (15037.6 mg) and vial 2 (15189.8 mg). Hereunder, vial 1 was evaporated in the Schlenk line for 5 minutes, and vial 2 was evaporated in the rotatory evaporator for 5 minutes with the heating bath set to 40 °C. The vials were weighted again with the intention of evaluate the loss of the product caused by the evaporation. As it is show in Table 8, there was an important loss after 5 minutes evaporating with both methods. Due to the small scale used in this reaction, we realized that the lost was more relevant in our conditions and the proposed system is not suitable for an accurate quantification. Thus, from this empirical observation we can conclude that: (a) probably the amount of coupling product formed during the stoichiometric reactions is higher than the one observed by ^1H NMR spectroscopy, and (b)

the comparison between experiments is not reliable since all the samples were not submitted to the same evaporation time.

Table 8. Evaporation test.

	Before evaporation	After evaporation	Lost product
Vial 1	15037.6 mg	15033 mg	4.6 mg
Vial 2	15189.8 mg	15189.2 mg	0.6 mg

4.5. C–Me bond-forming reaction from alternative **1_{DG-I}** systems

In order to tackle the detected loss of mass-balance during the work-up process and aiming to obtain an accurate quantification of the C–Me bond-forming reactions, we decided to explore the methylation reaction using an alternative **1_{DG-I}** complex. In particular, we targeted **1_{ppy-I}** based on its easy accessibility via oxidative addition,^{2a} the high yield observed for the methylation of 2-phenylpyridine in the scope reported by Ackermann and co-workers (Figure 17),¹⁶ and the higher molecular weight of the resulting methylated product.

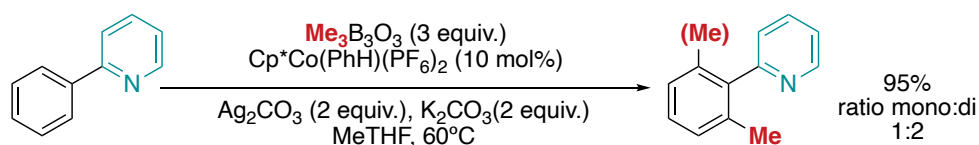
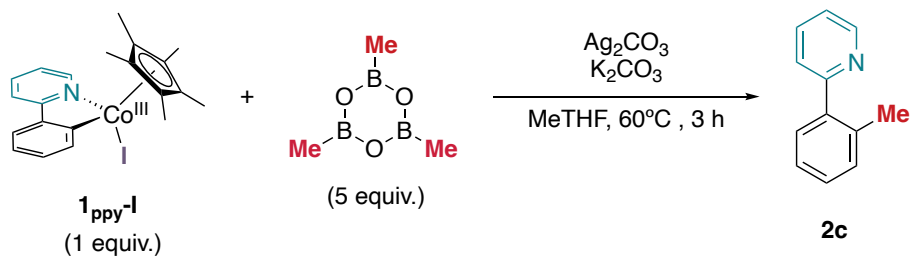


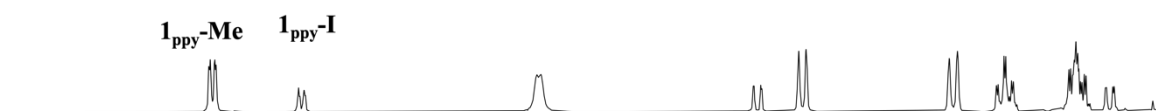
Figure 17. Methylation of 2-phenylpyridine reported by Ackermann and co-workers (reference 16).

We initiated our experiments **1_{ppy-I}** by establishing the feasibility of the C–C coupling under the most promising experimental results gathered for **1_{ald-I}**, using MeTHF as solvent. A crimped vial charged with **1_{ppy-I}**, trimethylboroxine, Ag₂CO₃ and K₂CO₃ was heated for 3 hours at 60 °C using MeTHF as solvent. Then, we filtered the reaction, evaporated the solvent and the crude reaction mixture was analyzed by ¹H NMR spectroscopy using CDCl₃ as solvent. In the spectrum shown in Figure 18, we observed unreacted cobalt (III) complex along with the formation of a new cobalt compound, that we assigned as **1_{ppy-Me}** based on the ¹H NMR spectral pattern. Apart of the aromatic signals that belong to the 2-ppy moiety, in the alkylic section we observe the signal of the Cp* ligand along with a signal that integrates as 3, that could belong to the methyl group bound to the cobalt metal center.

This contrasts with the results obtained with **1_{ald-I}**, where we could not observe the formation of any new species. The use of **1_{ppy-I}** under the conditions afforded the formation of **1_{ppy-Me}** and **1_{ppy-I}** in a ratio 73:27.



(a)



(b)

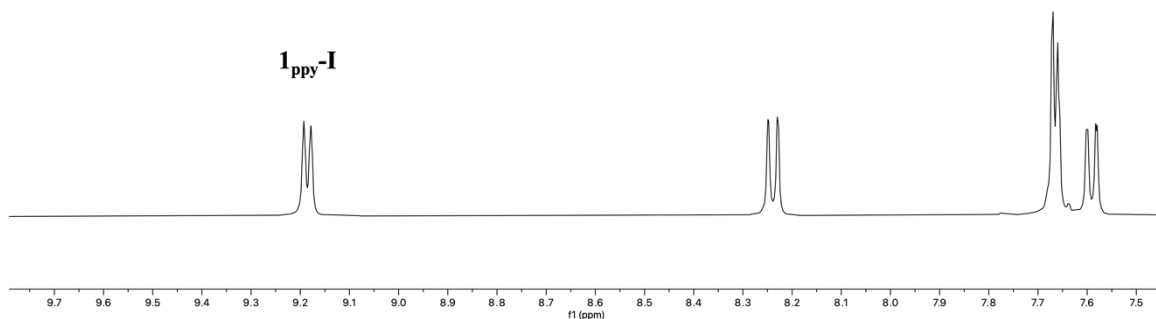


Figure 18. ^1H NMR spectra of the C–H methylation with **1_{ppy-I}**. Additives: (a) Ag_2CO_3 and K_2CO_3 (Entry1). Reference NMR spectra of: (b) **1_{ppy-I}**.

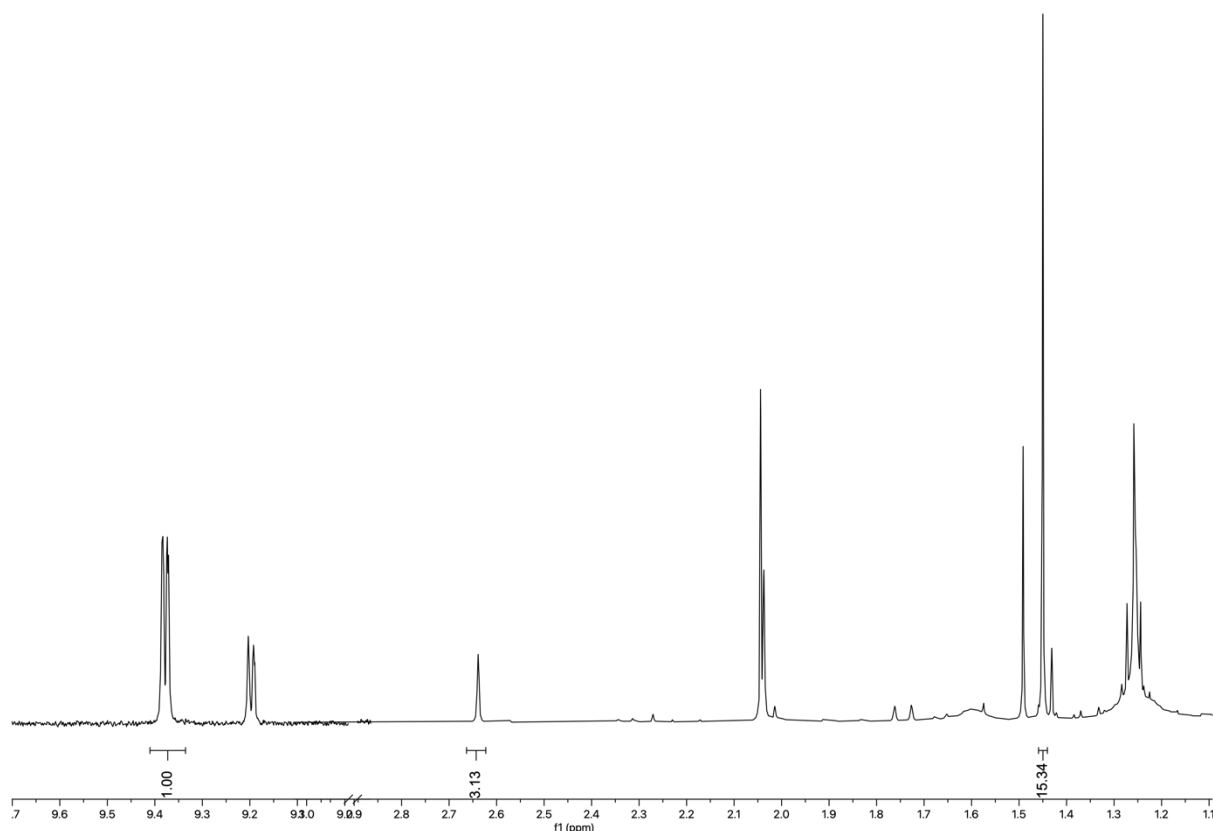
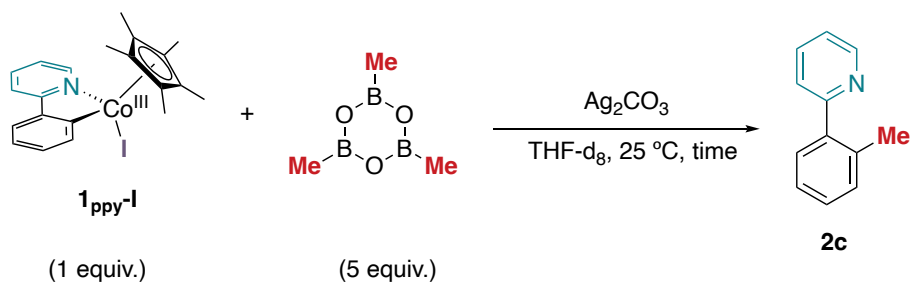


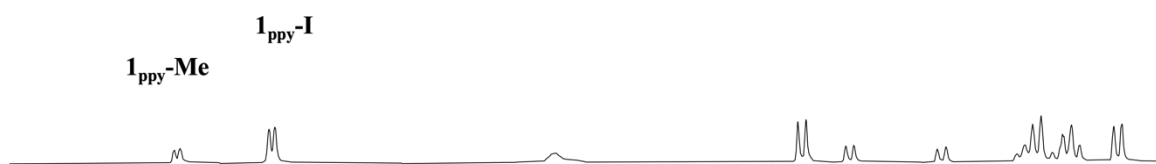
Figure 19. ^1H NMR spectra of the C–H methylation with **1_{ppy-I}** and **1_{ppy-Me}** product.

As shown for **1_{ald-I}**, we tried to isolate **1_{ppy-Me}** by the treatment of **1_{ppy-I}** and methyl lithium in THF at $-78\text{ }^\circ\text{C}$ for 1 hour, and then gradually warming to room temperature. Next, the solvent was carefully evaporated and measured by ^1H NMR spectroscopy in CDCl_2 . Unfortunately, we only observed the unreacted starting material, **1_{ppy-I}**.

Despite we could not synthesize an authentic sample of **1_{ppy-Me}** using MeLi, we explored whether the new observed species could belong to **1_{ppy-Me}**, by monitoring the stoichiometric reaction using ^1H NMR spectroscopy. We recorded different NMR spectra of the reaction between **1_{ppy-I}** and trimethylboroxine, in the presence of Ag_2CO_3 at room temperature using $\text{THF-}d_8$ as solvent. After 1h, we observed **1_{ppy-Me}** / **1_{ppy-I}** in a ratio 1:3. Gratifyingly, we observed that after 3 hours, the new peak that we assigned to **1_{ppy-Me}** grows, obtaining a ratio 1:2.



(a)



(b)

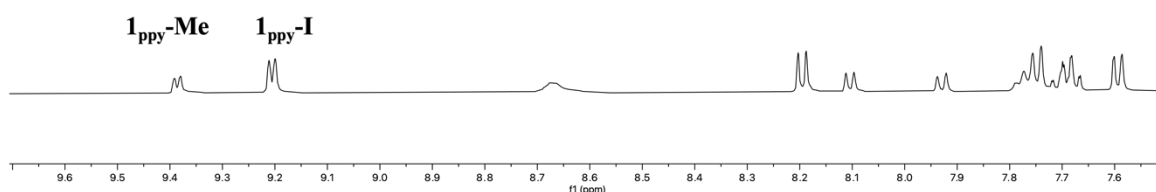


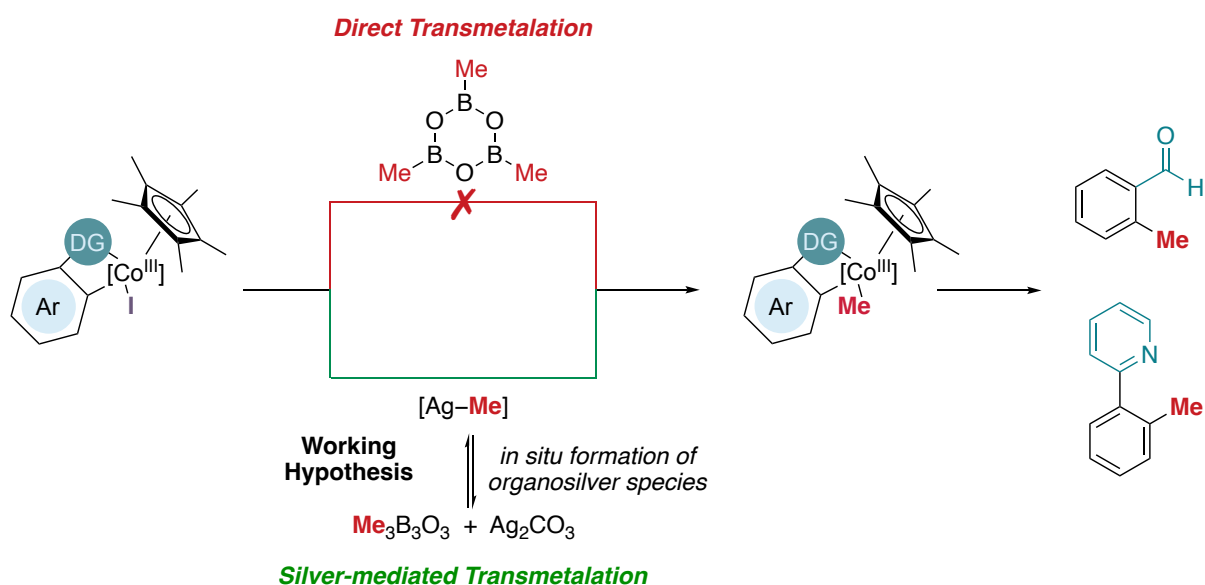
Figure 20. ^1H NMR spectra of the monitoring of C–H methylation with $\text{1}_{\text{ppy-I}}$. Time: (a) 1 hour; (b) 3 hours.

Overall, these experimental outcomes disclosed in the work strongly suggest that the nature of the directing group has a direct impact on the formation of the $\mathbf{1}_{\text{DG-Me}}$ and the subsequent coupling product. With aldehyde model system we could not observe the formation of any transient species and only product is detected under the investigated reaction conditions. In sharp contrast, with the 2-ppy system, due to the slower rate of the combined transmetalation and reductive elimination process, we can observe the formation of a new species that disappears along time to afford the coupling product. All the collected experimental evidences indicate that this transient species is the resulting cobaltacycle, $\mathbf{1}_{\text{DG-Me}}$, that would be formed after the transmetalation step.

5. Conclusions

The main objective of this Bachelor Thesis was to enhance our understanding of the mechanistic aspects of Cp*Co-catalyzed nucleophilic C–H functionalization couplings using as touchstone the synthetic protocol reported by the Ackermann and co-workers. From our stoichiometric experiments we can conclude:

- **1_{ald-I}** and **1_{ppy-I}** undergo transmetalation and reductive elimination under similar the reaction conditions to the ones reported by Ackermann.
- The selection of the initial cobalt precursor is crucial for ensuring reliable experimental data. We have observed that when using **1_{ald-I}** as starting material, the corresponding methylated organic product is volatile under the conditions we used to treat the reactions, leading to inaccurate quantifications. We have addressed this problem by using **1_{ppy-I}**, that affords a organic product of higher molecular weight and boiling point.
- The transmetalation step using only trimethylboroxine as transmetalating agent is not efficient and it is necessary the presence of Ag₂CO₃ to increase the formation of the coupling product. This suggests that an *in situ* generated Ag–Me species could be responsible of the transmetalation reaction under catalytic conditions.
- Despite the isolation of the hypothetical methylated cobaltacycle could not we achieved in this work, when we used **1_{ppy-I}**, the formation of a new species that seems to be **1_{ppy-Me}** is observed. Due to time constraints, we could not fully investigate if the reductive elimination step occurs via directed coupling from cobalt(III) species.



6. Outlook

Regarding the conclusions extracted from this work, several suggestions are proposed for further investigation and exploration of this system.

- Considering the limitations of the quantification with **1_{ald-I}** system and the desired product **2a**, it is recommended to explore a new quantification methodology that can overcome the challenges associated with product loss during workup and provide a more convenient and straightforward approach for quantification.
- To gain a deeper understanding of the mechanisms involved, as well as to investigate the impact of different directing groups, it is suggested to expand the scope of the studied system to include other directing groups. This expansion would provide valuable information and insights into the underlying mechanisms, while also allowing for a comprehensive exploration of the effects of different directing groups employed in the reaction.
- Perform a quantification study of the **1_{ppy-I}** system to evaluate both the yield and effectiveness of the system. This study aims to provide a detailed analysis of the quantitative aspects of the reaction, including the determination of the yield.
- Isolate and characterize the **1_{ppy-Me}** intermediate, as it will provide significant information regarding crucial steps such as transmetallation and reductive elimination, as well as the role of various additives involved in the process.

7. Experimental section

7.1. General procedures

All the experiments were carried out within an argon-filled glovebox (mBraun Unilab 4420) with concentrations of O₂ and H₂O < 0.1 ppm as well as using Schlenk techniques under argon atmosphere when it was required.







All the glassware was previously oven-dried at 100 °C overnight and cooled under vacuum. NMR spectra were carried out on a Bruker 400 MHz or 500 MHz instrument. Chemical shifts for ¹H nuclei are reported in parts per million (ppm) relative tetramethylsilane (TMS) with the residual solvent peaks serving as an internal reference.

To indicate multiplicities were used the following notations: singlet (s), broad signal (bs), doublet (d), doublets of doublets (dd), doublet of doublet od doublets (ddd), double of triplets (dt), double of doublet of quarters (ddq), triplets (t), triplets of doublets (td) and multiplet (m).

7.2. Materials and methods

Commercially available reagents 1,2,3,4,5-pentamethylcyclopentadiene, ⁿBuLi, CoCl₂, Zn powder, 2-iodobenzaldehyde, o-I-2-Phenylpyridine, 2-phenylpyridine, AgSbF₆, Ag₂CO₃, trimethylboroxine, K₂CO₃, MeLi, KOAc, triphenylboroxine, potassium methyltrifluoroboronate, methyl boronic acid pinacol ester, vinyltrimethylsilane.

Table 9. Most employed reagents

Reactive	Purity	Toxicological information
2-iodobenzaldehyde	97%	
2-phenylpyridine	-	
Ag ₂ CO ₃	99%	
Trimethylboroxine	99%	
K ₂ CO ₃ ,	99%	
MeLi	1.6 M Et ₂ O	

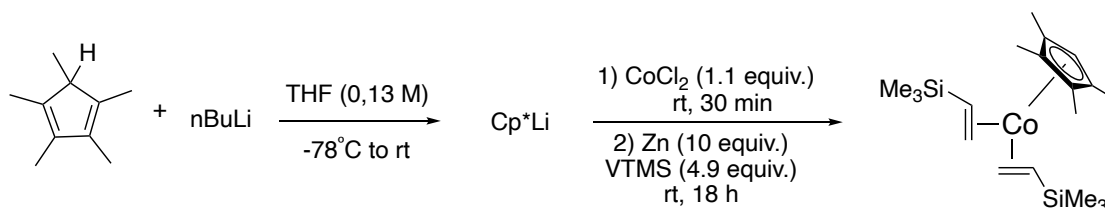
In order to manipulate all the reagents, it is mandatory to wear gloves, protective goggles and lab coat. Apart from the protection mentioned before, to manage safely the compounds is necessary to consider these preventive measures:

- 2-iodobenzaldehyde: Avoid breathing dust/ fume/ gas/ mist/ vapors/ spray.
- 2-phenylpyridine: Avoid breathing dust/ fume/ gas/ mist/ vapors/ spray.
- Ag₂CO₃: Avoid release to the environment.
- K₂CO₃: Avoid breathing dust.
- Trimethylboroxine: Keep away from heat, hot surfaces, sparks, open flames and other ignition sources.
- MeLi: Keep away from heat/ sparks/ open flames/ hot surfaces. Do not allow contact with air. Keep away from any possible contact with water, because of violent reaction and possible flash fire. Handle under inert gas. Protect from moisture.

The used solvents (THF, DCM, MeCN, Et₂O) were obtained from a solvent purification system (SPS-400, Innovative Technology) and stored under argon atmosphere. MeTHF was dried with activated 4 Å molecular sieves and it was stored under argon atmosphere.

7.3. Synthesis of cobalt species

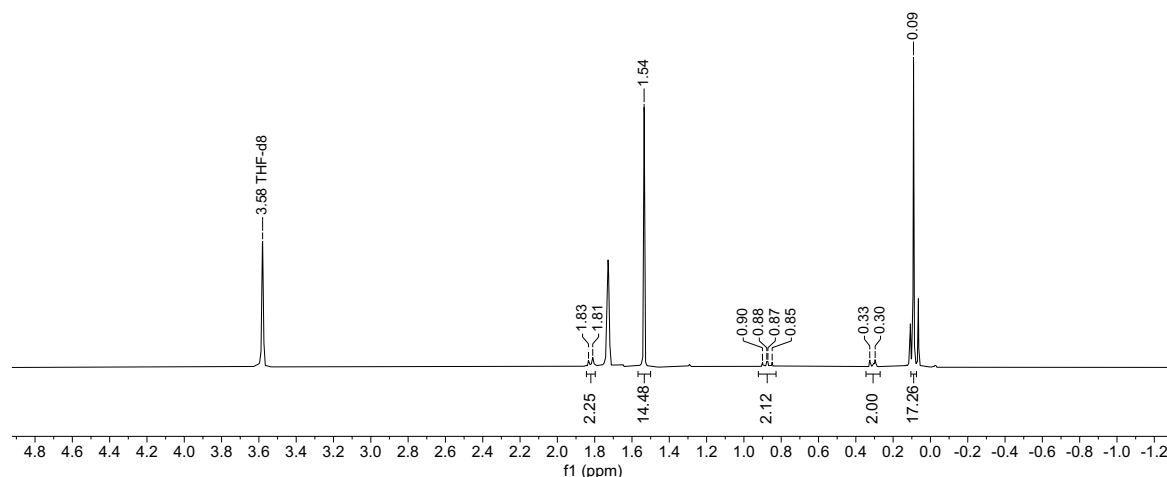
7.3.1. Synthesis and characterization of Cp*Co(VTMS)₂



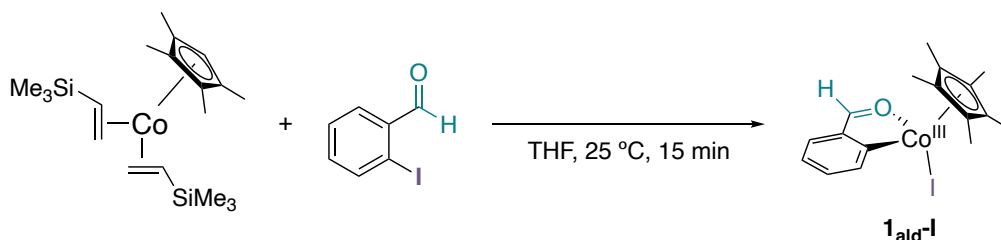
Under inert atmosphere, dried and degassed THF (30 mL) was added to an oven-dried Schlenk. Then, 1,2,3,4,5- pentacyclopentadiene (659 μ L, 4 mmol, 1 equiv.) was added, and the Schlenk was cooled to -78 °C. A 1.6 M solution of ⁿBuLi in ⁿhexane (2.75 mL, 4.4 mmol, 1.1 equiv.) was slowly charged to the Schlenk. The reaction was taken out of the acetone/dry ice bath and was left stirring until it reaches room temperature for 2 hours. Afterwards, CoCl₂ (572.3 mg, 4.4 mmol, 1.1 equiv.) and 30 mL of degassed THF we added to a separate Schlenk. The cobalt solution was cannula-transferred into Cp*Li Schlenk, and the reaction was stirred at room temperature for 30 minutes. Then, vinyltrimethylsilane (2.93 mL, 20 mmol, 4.9 equiv.) is added into the Schlenk and the solution is stirred for 5 minutes. The mixture was cannula-transferred into a Schlenk charged with Zn powder (2616 mg, 40 mmol, 10 equiv.) and the reaction is left under stirring for 18 hours at room temperature. The reaction was transferred and filtered through a cannula to a new dried Schlenk. The solvent was evaporated and the resulting solid was dissolved in hexane and filtered through a cannula to another Schlenk. Finally, the solvent was evaporated and the final product was obtained (853.1 mg, 55% yield).

¹H NMR (500 MHz, THF-*d*₈) δ 1.82 (d, J = 11.4 Hz, 2H), 1.54 (s, 15H), 0.87 (dd, J = 14.5, 11.5 Hz, 2H), 0.31 (d, J = 14.5 Hz, 2H), 0.09 (s, 18H).

^1H NMR spectrum at 298 K in THF- d_8



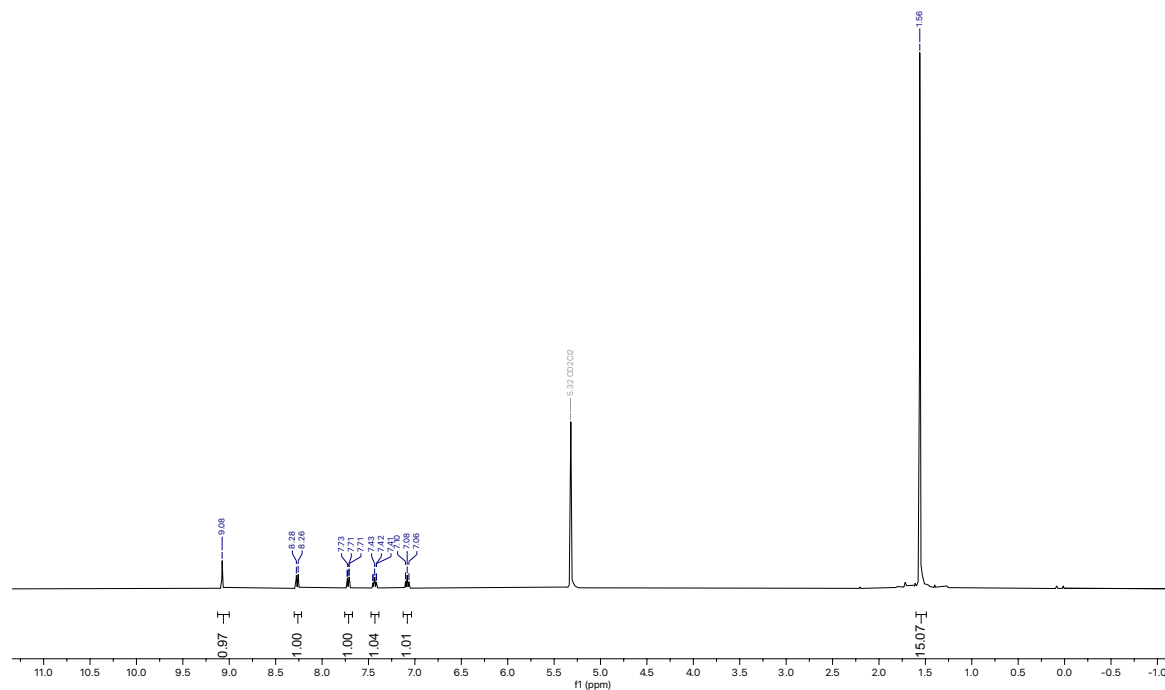
7.3.2. Synthesis and characterization of $1_{\text{ald-I}}$



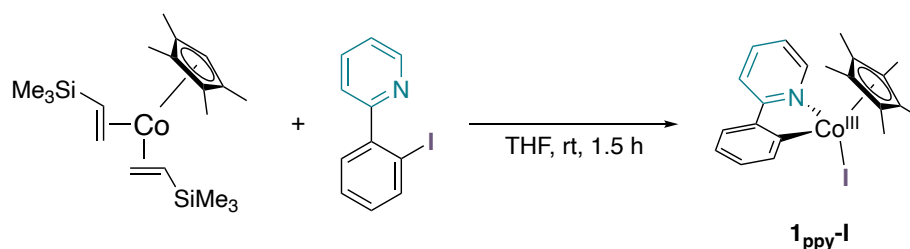
Inside an argon-filled glovebox, 2-iodobenzaldehyde (294 mg, 1.27 mmol, 1.1 equiv.) and previously-synthesized $\text{Cp}^*\text{Co}(\text{VTMS})_2$ (500 mg, 1.27 mmol, 1.1 equiv.) and 5 mL of THF were added to an oven-dried Schlenk. The reaction is stirred at room temperature for 15 minutes. Then, the solvent is evaporated, the resulting solid was dissolved in 5 mL of DCM and the solution was filtered through a PTFE syringe filter. The solvent is evaporated and the resulting solid was washed with 10 mL hexane. Finally, the product is dried under reduced pressure and the desired cobaltacycle is obtained (348 mg, 64% yield).

$^1\text{H NMR}$ (400 MHz, CD_2Cl_2) δ 9.08 (s, 1H), 8.27 (d, $J = 7.8$ Hz, 1H), 7.72 (dd, $J = 7.6, 1.5$ Hz, 1H), 7.48 – 7.39 (m, 1H), 7.08 (t, $J = 7.4$ Hz, 1H), 1.56 (s, 15H).

$^1\text{H NMR}$ spectrum at 298 K in CD_2Cl_2



7.3.3. Synthesis and characterization of **1_{ppy-I}**

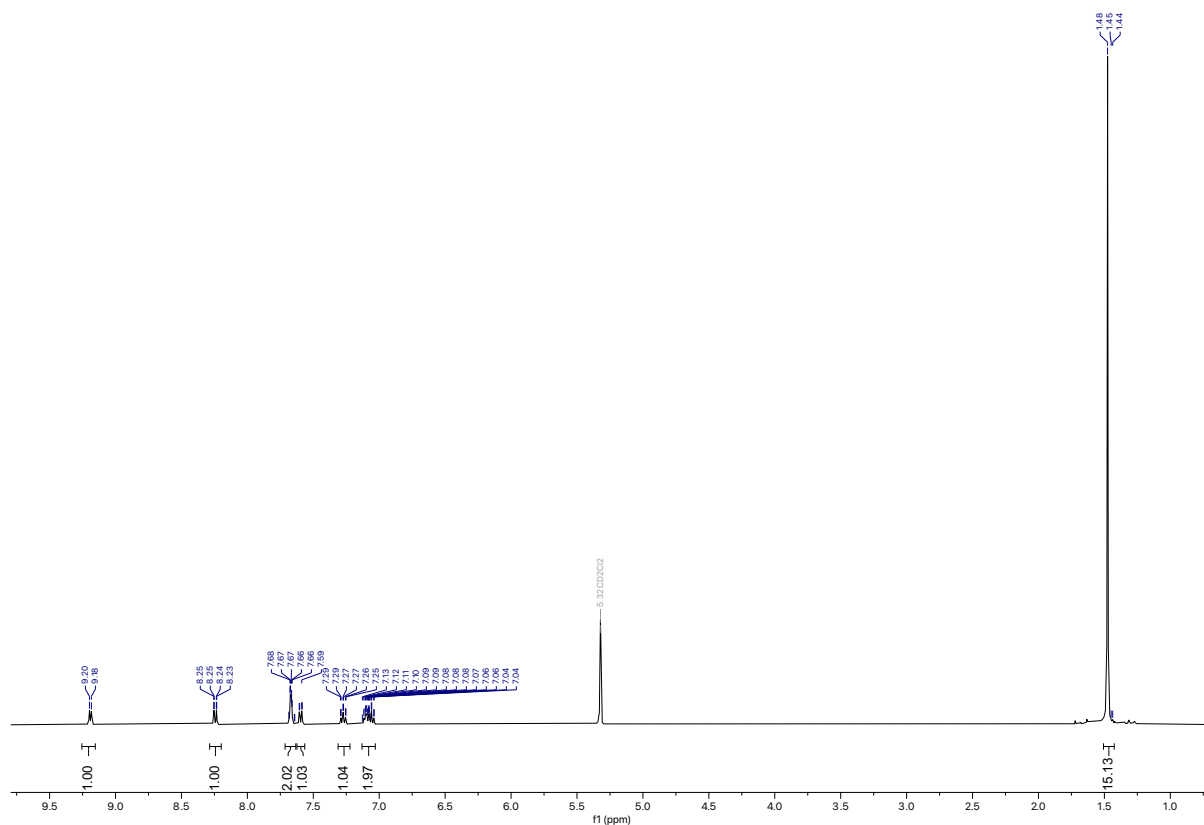


Inside an argon-filled glovebox, $\text{Cp}^*\text{Co}(\text{VTMS})_2$ (478 mg, 1.21 mmol, 1 equiv.) was charged in an oven-dried Schlenk and taken out of the glovebox. 15 mL of degassed THF were added. Thereafter, a solution of 2-(2-iodophenyl)pyridine (340 mg, 1.21 mmol, 1 equiv.) in 10 mL of degassed THF was added to the Schlenk flask and the mixture was stirred for 1.5 hours at room temperature. The solvent was removed under vacuum and the remaining solid was dissolved in DCM and cannula-filtered to another Schlenk flask. Then, DCM was removed under vacuum and the solid was dried on the line. The solid was dissolved again in DCM,

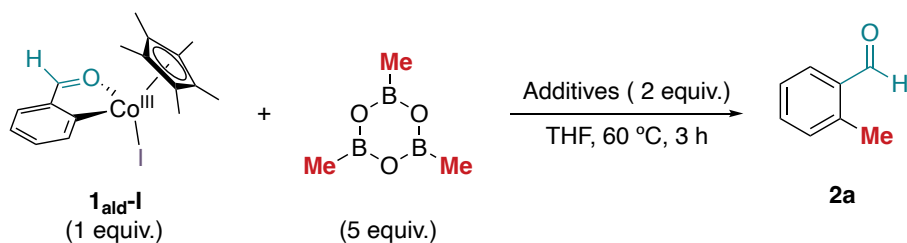
filtered through a celite plug and a PTFE syringe filter. The solvent was removed under vacuum and the product was obtained (346.5 mg, yield: 60%).

$^1\text{H NMR}$ (400 MHz, CD_2Cl_2) δ 9.19 (d, $J = 5.8$ Hz, 1H), 8.24 (dd, $J = 7.7, 1.2$ Hz, 1H), 7.71 – 7.62 (m, 2H), 7.60 (dd, $J = 7.6, 1.5$ Hz, 1H), 7.27 (td, $J = 7.4, 1.5$ Hz, 2H), 7.15 – 7.02 (m, 2H), 1.48 (s, 15H).

$^1\text{H NMR}$ spectrum at 298 K in CD_2Cl_2



7.4. Initial mechanistic studies

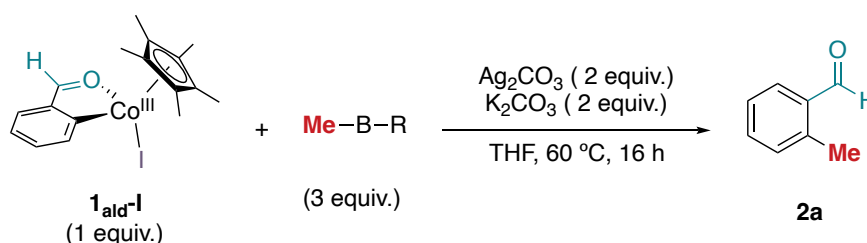


Inside an argon-filled glovebox, 1ald-I (4.26 mg, 0.01 mmol, 1 equiv.), $\text{Me}_3\text{B}_3\text{O}_3$ (7 μL , 0.05 mmol, 5 equiv.), the required additives (0.02 mmol, 2 equiv.) and non-deuterated THF (0.3 mL) were charged in a screw-cap NMR tube that contains a $\text{DMSO-}d_6$ capillary. The tube was

heated at 60°C for 3 hours in a oil bath. ¹H-NMR analysis was performed to confirm the reaction outcome.

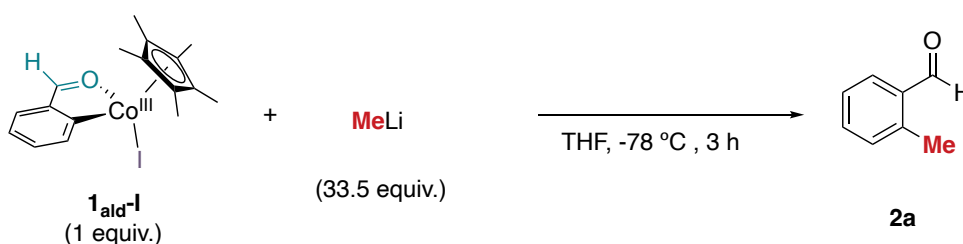
Entry	Additives	Ratio (2a:1 _{ald-I})
1	None	0:100
2	K ₂ CO ₃ (2.76 mg)	8:92
3	Ag ₂ CO ₃ (5.52 mg)	57:43
4	Ag ₂ CO ₃ (5.52 mg) and K ₂ CO ₃ (2.76)	21:79

7.5. Exploration of additional methylating sources



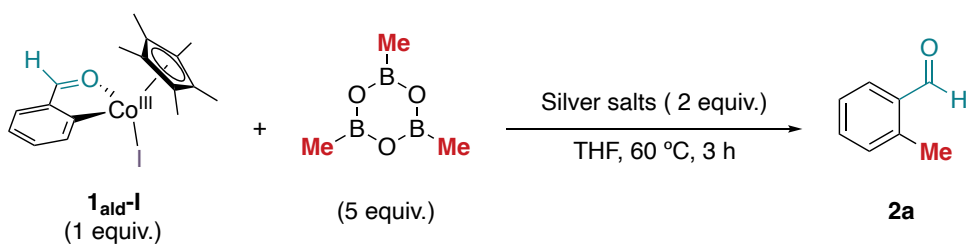
Inside an argon-filled glovebox, the **1_{ald-I}** (8.53mg, 0.02 mmol, 1 equiv.), the required methyl source (0.03 mmol, 3 equiv.), K₂CO₃ (2.76 mg, 0.02 mmol, 2 equiv.), Ag₂CO₃ (5.52 mg, 0.02 mmol, 2 equiv.) and 0.6 mL of THF were added to a crimped vial. The vial was taken out of the glovebox and stirred at 60 °C for 16 hours. The crude was filtered through a celite and silica pad. The reaction was measured by ¹H-NMR in CD₂Cl₂.

Entry	Methyl source	Ratio (2a:1 _{ald-I})
1	MeBpin (7.7 μL)	0:100
2	MeBF ₃ K (7.32 mg)	59:41



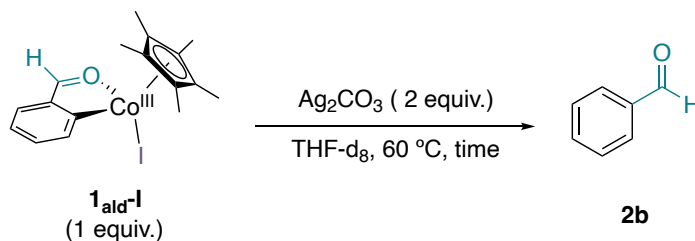
Inside an argon-filled glovebox, the **1_{ald-I}** (8.53mg, 0.02 mmol, 1 equiv.), and 0.5 mL of THF were added in a Schlenk. The Schlenk was taken out of the glovebox and the MeLi (20μL, 0.67 mmol, 33.5 equiv) was added. The mixture was stirred at -78 °C for 1 hour and after 1 hour, was stirred at room temperature for 2 hours. The solvent was evaporated and measured by ¹H-NMR in CD₂Cl₂.

7.6. The effect of silver salts



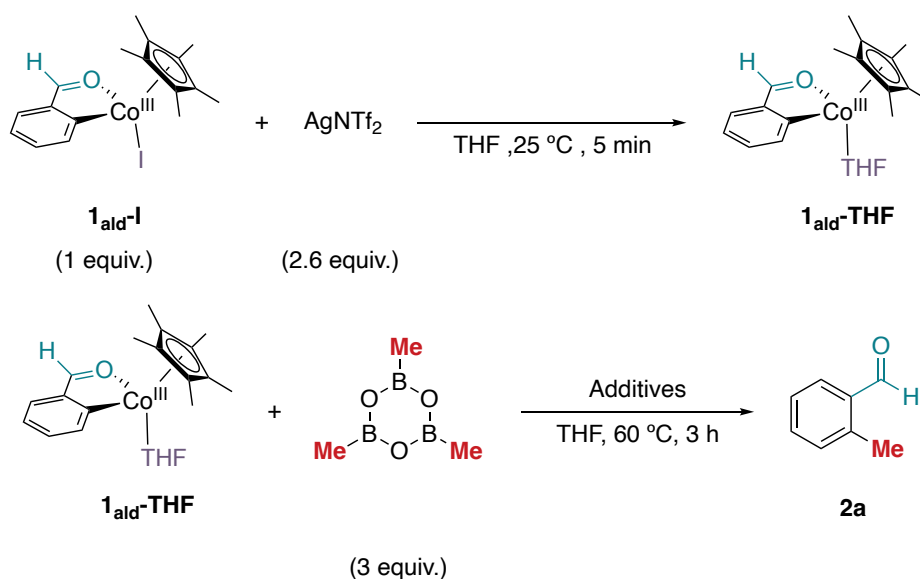
Inside an argon-filled glovebox, **1_{ald-I}** (4.26 mg, 0.01 mmol, 1 equiv.), Me₃B₃O₃ (7 μL, 0.05 mmol, 5 equiv.), silver salt (0.02mmol, 2 equiv.) and THF (0.3 mL) were charged in a screw-cap NMR tube that contains a DMSO-*d*₆ capillary. ¹H NMR was measured once all the substrates were added (15 minutes, rt) and was checked again after 3 hours stirring at 60°C in an oil bath. Then, the solution was filtered through a celite and silica pad and a final ¹H NMR measurement was performed in 0.5 mL of CDCl₃.

Entry	Silver sources	Ratio (2a:1 _{ald-I})
1	Ag ₂ CO ₃ (5.52 mg)	57:43
2	AgSbF ₆ (6.87 mg)	17:83
3	AgOAc (3.34 mg)	32:68
4	AgBF ₄ (3.89 mg)	Decomposition



Inside an argon-filled glovebox, **1_{ald-I}** (4.26 mg, 0.01 mmol, 1 equiv.), silver salt Ag₂CO₃ (5.52 mg, 0.02 mmol, 2 equiv.) and THF-*d*₈ (0.3 mL) were charged in a screw-cap NMR tube. ¹H NMR was measured after heating the tube at 60 °C for 1 and 3 hours.

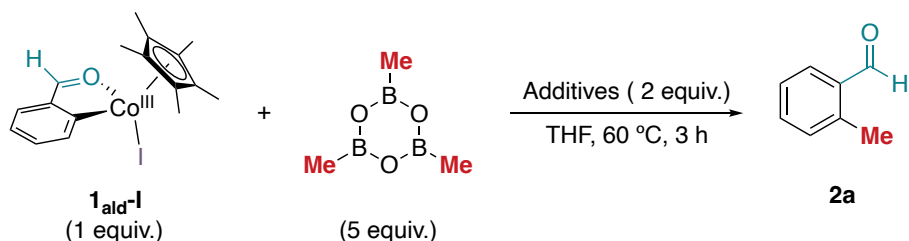
Entry	Time	Ratio (2b : 1_{ald-I})
1	1 hour	0:100
2	3 hours	30:70



Inside an argon-filled glovebox, **1_{ald-I}** (8.52 mg, 0.02 mmol, 1 equiv.), AgNTf₂ (8.47 mg, 0.05 mmol, 2.6 equiv.) and THF (0.6 mL) were charged into a vial. The reaction was left stirring for 5 minutes. The mixture was filtered through a PTFE syringe filter and charged into a crimped vial. Then, additives were added to the vial. The vial was taken out of the glovebox, and the mixture was stirred and heated at 60 °C for 3 hours. Then, the solution was filtered through a celite and silica pad and ¹H NMR measurement was performed in 0.5 mL of CDCl₃.

Entry	Reagents	Ratio (2a : 1_{ald-I})
1	Me ₃ B ₃ O ₃ (8.4 μL)	0:100
2	Ag ₂ CO ₃ (11 mg) & Me ₃ B ₃ O ₃ (8.4 μL)	30:70

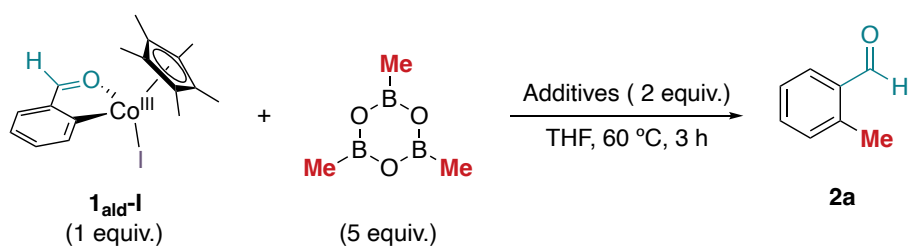
7.7. The effect of the bases



Inside an argon-filled glovebox, **1ald-I** (4.26 mg, 0.01 mmol, 1 equiv.), $\text{Me}_3\text{B}_3\text{O}_3$ (7 μL , 0.05 mmol, 5 equiv.), the required base (0.02 mmol, 2 equiv.), and THF (0.3 mL) were charged in a crimped vial. The vial was taken out of the glovebox and mixture was stirred for 3 hours at 60 °C. Then, the solution was filtered through a celite and silica pad and ^1H NMR measurement was performed in 0.5 mL of CDCl_3 .

Entry	Additives	Ratio (2a:1ald-I)
1	K_2CO_3 (2.76 mg)	8:92
2	KOAc (1.96 mg)	0:100

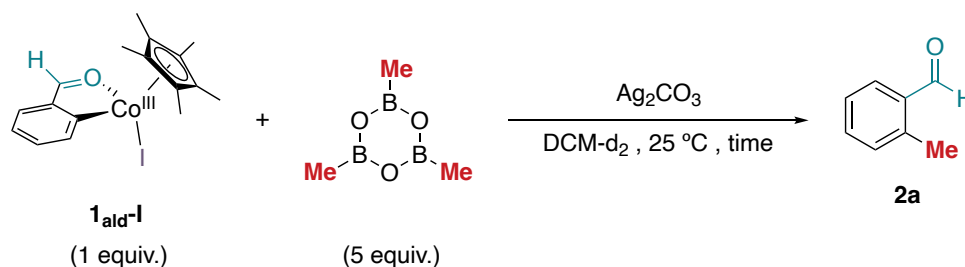
7.8. Methylation quantification



Entry	Additives	NMR yield
1	Ag_2CO_3 and K_2CO_3	25%
2	Ag_2CO_3	14%

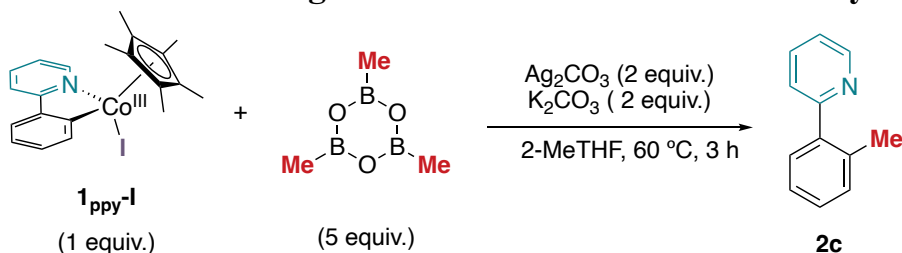
Inside an argon-filled glovebox, **1ald-I** (4.26 mg, 0.01 mmol, 1 equiv.), $\text{Me}_3\text{B}_3\text{O}_3$ (7 μL , 0.05 mmol, 5 equiv.), the required additives (0.02 mmol, 2 equiv.) and 0.3 mL of THF were added to a crimped vial. The tube was heated at 60°C for 16 hours in a sand bath. Then, the

solution was filtered through a celite and silica pad. For the quantification, were added 7.1 mg and 7.7 mg of 1,3,5- trimethoxybenzene for **Entry 1** and **Entry 2** respective conditions. ^1H NMR measurement was performed in 0.5 mL of CDCl_3 .

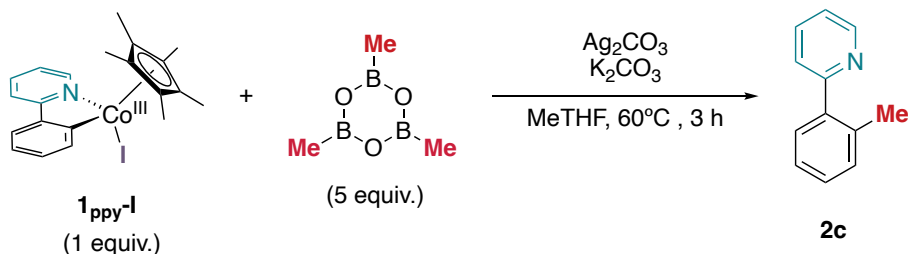


Inside an argon-filled glovebox, **1ald-I** (4.26 mg, 0.01 mmol, 1 equiv.), $\text{Me}_3\text{B}_3\text{O}_3$ (7 μL , 0.05 mmol, 5 equiv.), Ag_2CO_3 (5.52 mg, 0.02 mmol, 2 equiv.) and CD_2Cl_2 (0.3 mL) were charged in a screw-cap NMR tube. ^1H NMR was monitored using ^1H NMR spectroscopy at room temperature.

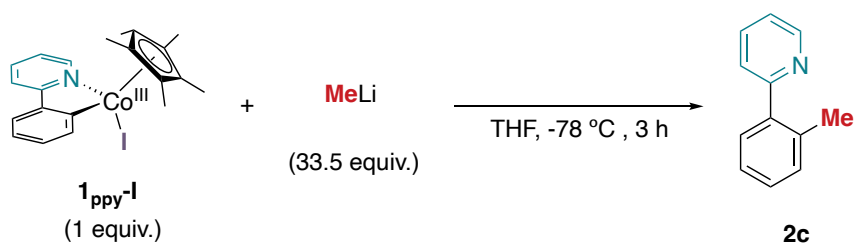
7.9. C–Me bond-forming reaction from alternative **1DG-I** systems



Inside an argon-filled glovebox, **1ppy-I** (4.76 mg, 0.01 mmol, 1 equiv.), $\text{Me}_3\text{B}_3\text{O}_3$ (7 μL , 0.05 mmol, 5 equiv.), K_2CO_3 (2.76 mg, 0.02 mmol, 2 equiv.), Ag_2CO_3 (5.52 mg, 0.02 mmol, 2 equiv.) and 2-MeTHF (0.3 mL) were charged in a crimped vial. The vial was taken out of the glovebox and stirred at 60 °C for 3 hours. The crude was filtered through a celite and silica pad. The crude was measured by ^1H -NMR in CDCl_3 .



Inside an argon-filled glovebox, **1ppy-I** (4.76 mg, 0.01 mmol, 1 equiv.), $\text{Me}_3\text{B}_3\text{O}_3$ (7 μL , 0.05 mmol, 5 equiv.), K_2CO_3 (2.76 mg, 0.02 mmol, 2 equiv.), Ag_2CO_3 (5.52 mg, 0.02 mmol, 2 equiv.) and THF-d_8 (0.3 mL) were charged in a screw-cap NMR tube. The vial was taken out of the glovebox and ^1H -NMR was measured through time.



Inside an argon-filled glovebox, the **1_{ppy-I}** (4.76 mg, 0.02 mmol, 1 equiv.), and 0.5 mL of THF were added in a Schlenk. The Schlenk was taken out of the glovebox and the MeLi (20 μL , 0.67 mmol, 33.5 equiv.) was added. The mixture was stirred at $-78\text{ }^\circ\text{C}$ for 1 hour .and after 1 hour, was stirred at room temperature for 2 hours. The solvent was evaporated and measured by $^1\text{H-NMR}$ in CD_2Cl_2 .

8. References and notes

- ¹ Sanjosé-Orduna, J.; Mudarra, A. L.; Martínez de Salinas, S.; Pérez-Temprano, M. H. *ChemSusChem* **2019**, *12*, 2882.
- ² (a) Sanjosé-Orduna, J.; Gallego, D.; Garcia-Roca, A.; Martin, E.; Benet-Buchholz, J.; Pérez-Temprano, M. H. *Angew. Chem. Int. Ed.* **2017**, *56*, 12137. (b) Sanjosé-Orduna, J.; Sarria Toro, J. M.; Pérez-Temprano, M. H. *Angew. Chem. Int. Ed.* **2018**, *57*, 11369. (c) Sanjosé-Orduna, J.; Benet-Buchholz, J.; Pérez-Temprano, M. H. *Inorg. Chem.* **2018**, *58*, 10569. (d) Martínez de Salinas, S.; Sanjosé-Orduna, J.; Odena, C.; Barranco, S.; Benet-Buchholz, J.; Pérez-Temprano, M. H. *Angew. Chem. Int. Ed.* **2020**, *59*, 6239. (e) López-Resano, S.; Martínez de Salinas, S.; Garcés-Pineda, F. A.; Moneo-Corcuera, A.; Galán-Mascarós, J. R.; Maseras, F.; Pérez-Temprano, M. H. *Angew. Chem. Int. Ed.* **2021**, *60*, 11217.
- ³ a) *Cross-Coupling Reactions: A Practical Guide*; Miyaura, N., (Ed.) in *Topics in Current Chemistry Series 2019*; Springer-Verlag Berlin Heidelberg, 2002. (b) Johansson Seechurn, C. C. C.; Kitching, M. O.; Colacot, T. J.; Snieckus, V. *Angew. Chem. Int. Ed.* **2012**, *51*, 5062. (c) *Metal-Catalyzed Cross-Coupling Reactions and More*, 1st ed.; de Meijere, A., Bräse, S., Oestreich, M. (Eds.); Wiley-VCH, 2014.
- ⁴ (a) *Organometallics as Catalysts in the Fine Chemical Industry*; Beller, M., Blaser, H.-U. (Eds.); Springer-Verlag Berlin Heidelberg, **2012**. (b) *Applied Cross-Coupling Reactions*; Nishihara, Y. (Ed.); Springer-Verlag Berlin Heidelberg, **2013**.
- ⁵ (a) Labinger, J. A.; Bercaw, J. E. *Nature* **2002**, *417*, 507; (b) Bergman, R. G. *Science* **1984**, *223*, 902. (c) Hartwig, J. F. *Acc. Chem. Res.* **2012**, *45*, 864; (d) Kuhl, N.; Hopkinson, M. N.; Wencel-Delord, J.; Glorius, F. *Angew. Chem. Int. Ed.* **2012**, *51*, 10236. (e) Yamaguchi, J.; Yamaguchi, A. D.; Itami, K. *Angew. Chem. Int. Ed.* **2012**, *51*, 8960. (f) Gensch, T.; Hopkinson, M. N.; Glorius, F.; Wencel-Delord, J. *Chem. Soc. Rev.* **2016**, *45*, 2900. (g) Gunsalus, N. J.; Koppaka, A.; Park, S. H.; Bischof, S. M.; Hashiguchi, B. G.; Periana, R. A. *Chem. Rev.* **2017**, *117*, 8521.
- ⁶Gandeepan, P.; Müller, T.; Zell, D.; Cera, G.; Warratz, S.; Ackermann, L. *Chem. Rev.* **2019**, *119*, 2192.
- ⁷<https://www.dailymetalprice.com/> accessed on 31/05/2023.
- ⁸Murahashi, S. *J. Am. Chem. Soc.* **1955**, *77*, 6403.
- ⁹(a) Colby, D. A.; Tsai, A. S.; Bergman, R. G.; Ellman, J. A. *Acc. Chem. Res.* **2012**, *45*, 814. (b) Song, G.; Li, X. *Acc. Chem. Res.* **2015**, *48*, 1020.
- ¹⁰Roe, D. M.; Maitlis, P. M. *J. Chem. Soc. A* **1971**, 3173.

- ¹¹Yoshino, T.; Ikemoto, H.; Matsunaga, S.; Kanai, M. *Angew. Chem. Int. Ed.* **2013**, *52*, 2207.
- ¹²Ikemoto, H.; Yoshino, T.; Sakata, K.; Matsunaga, S.; Kanai, M. *J. Am. Chem. Soc.* **2014**, *136*, 5424.
- ¹³Barranco, S.; Zhang, J.; López-Resano, S.; Casnati, A.; Pérez-Temprano, M. H. *Nat. Synth.* **2022**, *1*, 841.
- ¹⁴Gensch, T.; Klauck, F. J. R.; Glorius, F. *Angew. Chem. Int. Ed.* **2016**, *55*, 11287.
- ¹⁵Liu, X. G.; Li, Q.; Wang, H. *Adv. Synth. Catal.* **2017**, *359*, 1942.
- ¹⁶Friis, S.D.; Johansson, M.J.; Ackermann, L. *Nat. Chem.* **2020**, *12*, 511.
- ¹⁷(a) Guillemard, L.; Kaplaneris, N.; Ackermann, L.; Johanson, M. J. *Nat. Rev. Chem.* **2021**, *5*, 522. (b) Zhang, L.; Ritter, T. *J. Am. Chem. Soc.* **2022**, *144*, 2399.
- ¹⁸Aynetdinova, D.; Callens, M. C.; Hicks, H. B.; Poh, C. Y. X.; Shennan, B. D. A.; Boyd, A. M.; Lim, Z. H.; Leitch, J. A.; Dixon, D. J. *Chem. Soc. Rev.* **2021**, *50*, 5517.
- ¹⁹(a) *Organotransition Metal Chemistry: From Bonding to Catalysis*, 1st ed.; Hartwig, J. F. (Ed.); Palgrave Macmillan, 2009. (b) *Organometallics in Synthesis, Third Manual*; Schlosser, M. (Ed.); Wiley, 2013. (c) *The Organometallic Chemistry of the Transition Metals*, 7th ed.; Crabtree, R. H. (Ed.); Wiley, 2019.
- ²⁰Mudarra, A. L.; Martínez de Salinas, S.; Pérez-Temprano, M. H. *Org. Biomol. Chem.* **2019**, *17*, 1655.
- ²¹Unpublished results by the Pérez-Temprano group.
- ²²We compared the obtained ¹H NMR spectra of the reaction with spectra of the initial **1_{ald-I}** and the spectra of pure **2a** and we confirmed the formation of the methylated aldehyde.
- ²³Due to the lack of further experiments with this nucleophilic source, we cannot conclude why we do not observe any organic or organometallic compound by ¹H NMR spectroscopy.
- ²⁴Campos, J.; López-Serrano, J.; Peloso, R.; Carmona, E. *Chem. Eur. J.* **2016**, *22*, 6432.
- ²⁵We have confirmed the assignment of the new peak as benzaldehyde by analyzing this commercially available reagent by NMR spectroscopy.
- ²⁶We observe the formation of additional unknown by-product at 10.6 ppm.